

DRAFT VERSION DECEMBER 22, 2017
Typeset using L^AT_EX **preprint** style in AASTeX61

FUNDAMENTAL PARAMETERS OF EIGHTY-SEVEN STARS FROM THE NAVY PRECISION OPTICAL INTERFEROMETER

ELLYN K. BAINES, J. THOMAS ARMSTRONG, HENRIQUE R. SCHMITT,¹
R. T. ZAVALA, JAMES A. BENSON, DONALD J. HUTTER,² CHRISTOPHER TYCNER,³ AND
GERARD T. VAN BELLE⁴

¹*Naval Research Laboratory, Remote Sensing Division, 4555 Overlook Ave SW, Washington, DC 20375*

²*U.S. Naval Observatory Flagstaff Station, 10391 W. Observatory Rd, Flagstaff, AZ 86001*

³*Central Michigan University, Department of Physics, 1200 S. Franklin St, Mt Pleasant, MI 48859*

⁴*Lowell Observatory, 1400 W. Mars Hill Rd, Flagstaff, AZ 86001*

ABSTRACT

We present the fundamental properties of 87 stars based on angular diameter measurements from the Navy Precision Optical Interferometer, 36 of which have not been measured previously using interferometry. Our sample consists of 5 dwarfs, 3 subgiants, 69 giants, 3 bright giants, and 7 supergiants, and span a wide range of spectral classes from B to M. We combined our angular diameters with photometric and distance information from the literature to determine each star's physical radius, effective temperature, bolometric flux, luminosity, mass, and age.

Keywords: stars: fundamental parameters, techniques: high angular resolution, techniques: interferometric

1. INTRODUCTION

Interferometry is ideally suited to measure the angular diameters of stars, from main-sequence dwarfs (e.g., Boyajian et al. 2012b) to giants (e.g., Wittkowski et al. 2001; Baines et al. 2016) to supergiants (e.g., van Belle et al. 2009; Wittkowski et al. 2017) to special cases such as carbon stars (van Belle et al. 2013), nearby solar-type stars (Kervella et al. 2017), Mira variable stars (Wittkowski et al. 2016), and so on. The direct measurements of these stars’ angular diameters are key to determining their fundamental properties such as their physical radii and effective temperatures. These measurements act as a vital check to assumptions inherent in stellar structure and evolution models.

Interferometric diameters touch many topics of scientific interest. To name a few, they tell us about stars like our Sun and what solar-type stars will become as they evolve (e.g., Bazot et al. 2011). They help determine the ages of stars with imaged companions, so we know whether those companions are older, cooler brown dwarfs or younger, hotter exoplanets (e.g., Baines et al. 2012; Jones et al. 2016). They act as a direct test of astroseismic relationships (e.g., Huber et al. 2012; Baines et al. 2014). They characterize exoplanet host stars, which is a vital step in understanding the nature of the companions (e.g., Ligi et al. 2012; Boyajian et al. 2015). Furthermore, with the release of *Gaia* parallaxes, the distance to these targets will be updated and improved (Lindegren et al. 2012). When their distances are more precisely determined, the stars’ physical radii are also more precisely known.

Interferometers have produced excellent survey results in the past, such as in van Belle et al. (1999), Nordgren et al. (1999), Mozurkewich et al. (2003), and Boyajian et al. (2013). This work represents the largest sample of interferometrically measured angular diameters for single stars to date. We present the 87 stars observed with the Navy Precision Optical Interferometer (NPOI) that have diameter measurements with errors of a few percent or, as in most cases, less. This paper in conjunction with the multiplicity study by Hutter et al. (2016) highlight the NPOI’s utility as a survey instrument. The stars cover most spectral types (B to M) and feature mostly giants (66) with 4 dwarfs, 4 subgiants, 5 bright giants, and 8 supergiants.¹ Table 1 lists each star’s identifiers, spectral type, V magnitude, parallax, and metallicity.

The paper is organized as follows: Section 2 discusses the NPOI and our observing process, including the selection and characterization of calibrator stars; Section 3 describes the visibility measurements, the angular diameter dependence on the calculated calibrator diameter, and how we determined various stellar parameters, including the bolometric flux, extinction, luminosity, effective temperature, radius, mass, and age for each target; Section 4 considers what conclusions we can draw from the sample with respect to instrumental performance and previous interferometric measurements (when they exist); and Section 5 summarizes our findings.

2. INTERFEROMETRIC OBSERVATIONS

2.1. *The Navy Precision Optical Interferometer*

The NPOI is an optical interferometer located on Anderson Mesa, AZ (see Armstrong et al. 1998 for the instrument description and Hummel et al. 2003 and Benson, Hummel, & Mozurkewich 2003 for details about the beam combiner). The NPOI consists of two nested arrays: the four fixed stations of the astrometric array (AC, AE, AW, and AN, which stand for astrometric center,

¹ These are based on *SIMBAD* spectral types with preference given to the first luminosity class if a range is given. We update these types later in the paper.

east, west, and north, respectively) that are clustered at the center of the array, and the stations of the imaging array. The latter are arranged along three arms with general north, east, and west orientations. Each arm has ten piers where a siderostat can be installed, which means the imaging array can be reconfigured as needed.

The NPOI currently has six imaging stations in operation (E3, E6, E7, W4, W7, and N3) and four more will be coming online in the near future (N6, N7, E10, and W10). The stations are labeled according to which arm they are on and how far away they are from the array center, with 1 being closest and 10 being farthest away. The current baselines, i.e., the distance between stations, range from 10 m to 97 m. When the E10 and W10 stations are commissioned, the NPOI will have the longest baseline of any optical interferometer at 432 m.

The NPOI uses a 12.5-cm diameter region of 50-cm siderostats in both the astrometric and imaging stations. We can combine light from any of the astrometric and imaging stations that are appropriate for our science goals, up to six stations at a time. The current magnitude limit is ~ 5.5 in the V -band under normal conditions ~ 6.0 in excellent conditions.²

We observed 87 stars from 2004 to 2016, a data set that totals over 100,000 calibrated data points. Table 2 lists the stars observed, the calibrators used, the dates, baselines, and number of observations. We used the “Classic” beam combiner that takes data over 16 spectral channels spanning 550 to 850 nm (Hummel et al. 2003; Hutter et al. 2016). Each observation consisted of a 30-second coherent (on the fringe) scan where the fringe contrast was measured every 2 ms. Every coherent scan was paired with an incoherent (off the fringe) scan that was used to estimate the additive bias affecting fringe measurements (Hummel et al. 2003). Scans were taken on one to five baselines simultaneously. Each coherent scan was averaged to a 1-second data point, and then to a single 30-second average. The dispersion of the 1-second data points estimated the internal uncertainties.

The NPOI’s data reduction package *OYSTER* was developed by C. A. Hummel³ and automatically edits data using the method described in Hummel et al. (2003). In addition to that process, we edited individual data points and/or scans that showed large scatter, on the order of 5σ or higher. This was more common in the channels corresponding to the short wavelengths, a long-standing feature in NPOI data, where the channels are narrower, the atmospheric effects are more pronounced, and the avalanche photodiode detectors have lower quantum efficiencies. Removing those short-wavelength scans did not affect the diameter measurements.

The NPOI uses an extensive laser metrology system to measure the three-dimensional motions of the baselines with respect to an Earth-fixed reference system and to determine the absolute wavelength reference (for details, see Hutter & Elias 2003). In order to characterize the stability of the wavelength scale calibration, the NPOI regularly measured the central wavelengths of all the spectrometer channels in a Fourier transform spectrometer mode starting in 2005. The measurements show the central wavelengths are stable with a 0.6 nm (0.1%) scatter (Hutter et al. 2016). For data prior to 2005, we incorporated a $\pm 0.5\%$ error in the wavelength scale. Only five stars include data from 2004, and of those stars only one (HD 172167) used only 2004 data and had an uncertainty $< 0.5\%$. We assigned a 0.5% error to its diameter to account for the uncertainty in the wavelength scale.

² The NPOI will soon receive 3 1-meter telescopes, which will improve the array’s sensitivity to $V = 9$.

³ www.eso.org/~chummel/oyster/oyster.html

2.2. Selection and Characterization of Calibrator Stars

The theoretical response of an interferometer for a point source is known. We chose small stars to act as those point-source calibrators, and observed them in sequence with our science target. When we know what the calibrator's visibility should look like, we can compare that to what we see. We corrected for the difference between the theoretical positions and observed data, which is caused mostly by atmospheric effects.

To estimate the calibrator stars' angular diameters, we created spectral energy distribution (SED) fits based on published *UBVRIJHK* photometric values obtained from the literature. We used plane-parallel model atmospheres (Castelli & Kurucz 2004) based on T_{eff} , surface gravity ($\log g$), and $E(B - V)$. The stellar models were fit to observed photometry after converting magnitudes to fluxes using Colina et al. (1996) for *UBVRI* and Cohen et al. (2003) for *JHK*. See Table 3 for the photometry, effective temperature (T_{eff}), $\log g$, and $E(B - V)$ used as well as the resulting angular diameters. This is a relatively simple SED fit, unlike the one described in Section 3.2. For calibrator stars, it is appropriate considering the insensitivity of the final target's angular diameter with regard to the calibrator's diameter (discussed further in Section 3.1). We compared our estimated diameters to those predicted by the *SearchCal* tool provided by JMMC (Chelli et al. 2016). The difference between the diameters was an average of only 8%.

We checked every calibrator star for binarity, variability, and rapid rotation. Some of the calibrators chosen featured one or more of those properties, but not to an extent that would affect the calibration process. For the calibrators used here, any binary separation was beyond the detection limit of the configuration used, while the oblateness due to rapid rotation and/or variability in visible wavelengths did not affect the SED fits.

The standard procedure when reducing NPOI data includes smoothing systematic variations in the measured visibilities for the calibrator according to time. We used a smoothing time of 80 minutes, since that was found to be the optimal value for angular diameter measurements as described in Hutter et al. (2016).

3. RESULTS

3.1. Angular Diameter Measurement

Interferometric diameter measurements use visibility squared (V^2). For a point source, V^2 is 1 and it is considered completely unresolved. A star is completely resolved when its V^2 reaches zero, but naturally a signal of zero is not easily measurable. For a uniformly-illuminated disk, $V^2 = [2J_1(x)/x]^2$, where J_1 is the Bessel function of the first order, $x = \pi B\theta_{\text{UD}}\lambda^{-1}$, B is the projected baseline toward the star's position, θ_{UD} is the apparent uniform disk angular diameter of the star, and λ is the effective wavelength of the observation (Shao & Colavita 1992). θ_{UD} results are listed in Table 4. The data are freely available in OIFITS form (Duvert et al. 2017) upon request.

A more realistic model of a star's disk includes limb-darkening (LD). If a linear LD coefficient μ_λ is used, then

$$V^2 = \left(\frac{1 - \mu_\lambda}{2} + \frac{\mu_\lambda}{3} \right)^{-1} \times \left[(1 - \mu_\lambda) \frac{J_1(x_{\text{LD}})}{x_{\text{LD}}} + \mu_\lambda \left(\frac{\pi}{2} \right)^{1/2} \frac{J_{3/2}(x_{\text{LD}})}{x_{\text{LD}}^{3/2}} \right]^2. \quad (1)$$

where $x_{\text{LD}} = \pi B\theta_{\text{LD}}\lambda^{-1}$ (Hanbury Brown et al. 1974b). We used T_{eff} , $\log g$ values, and metallicity ([Fe/H]) values from the literature with a microturbulent velocity of 2 km s^{-1} to obtain μ_λ from

Claret & Bloemen (2011). We used the ATLAS model in the R -band, since that waveband most closely matched the central wavelength of the NPOI’s bandpass. The T_{eff} , $\log g$, [Fe/H], and μ_{λ} used and resulting θ_{LD} measurements are listed in Table 4. Figure 1 shows the θ_{LD} fit for HD 432 as a representative example. The remaining plots are included in the supplementary material of the *Astronomical Journal*.

The standard NPOI data reduction sequence incoherently averages the 2 ms data frames to produce 1 s “points,” and then averages the points to produce a scan. This two-step averaging procedure is performed separately for each baseline and wavelength channel. In addition to V^2 , it also yields an estimate of the measurement error for the scan based on the variance of the points within the scan.

However, the uncertainty in a stellar diameter can be significantly underestimated if we feed the V^2 and the measurement error estimates into a standard χ^2 minimization routine without regard to the correlations within a scan. In particular, a calibration error, which can arise naturally because the calibration-star scan is taken at a different time, affects the visibilities for all the baselines and channels within a scan.

To produce an estimate of the diameter uncertainty, we use a modified bootstrap Monte Carlo method devised by Tycner et al. (2010), in which we create a large number of synthetic datasets by selecting scans, rather than individual data points, at random. The width of the distribution of diameters fit to these datasets becomes our measure of the uncertainty in the diameter (see Figure 2). This uncertainty estimate can be as much as an order of magnitude greater than an estimate based only on the within-scan measurement errors.

In order to test the robustness of the calibration process, we changed the calibrator diameter by $\pm 10\%$ and recalculated target angular diameters. The resulting change in the target’s diameters (θ_{DIFF}) was $< 1\%$ for 72 stars and between 1% and 2% for 12 stars. The remaining stars where $\theta_{\text{DIFF}} \geq 3\%$ are:

HD 109358: $\theta_{\text{DIFF}} = 3\%$, which is larger than the measured angular diameter percent error (σ_{LD}) of 1.7% . We increased σ_{LD} to 3% to account for θ_{DIFF} .

HD 120136: This is the second smallest star in the sample, with $\theta_{\text{LD}} = 0.822$ mas. Its σ_{LD} was measured to be 4.6% , which is less than $\theta_{\text{DIFF}} = 6\%$. We increased σ_{LD} to 6% to account for θ_{DIFF} .

HD 120315: $\theta_{\text{DIFF}} = 4\%$, which is far less than $\sigma_{\text{LD}} = 15\%$. We left the larger σ_{LD} intact.

In most cases (73 out of 87), σ_{LD} was larger than θ_{DIFF} . Of the 14 remaining stars, 12 stars had $\theta_{\text{DIFF}} < 1\%$, and the two remaining stars had $\theta_{\text{DIFF}} \sim 1\%$. This demonstrated that the assumed calibrator angular diameter of 5% is reasonable, considering that increasing that uncertainty to 10% had so little effect on the final angular diameters of the target stars.

3.2. Stellar Radius, Luminosity and Effective Temperature

For each target, the parallax from van Leeuwen (2007)⁴ was converted into a distance and combined with our measured diameters to calculate the physical radius R . In order to determine each star’s luminosity L and T_{eff} , we created SED fits using photometric values published in Ljunggren & Oja (1965), McClure & Forrester (1981), Olsen (1993), Jasevicius et al. (1990), Golay (1972), Häggkvist & Oja (1970), Kornilov et al. (1991), Eggen (1968), Johnson et al. (1966), Cutri et al. (2003), and Gezari et al. (1993) as well as spectrophotometry from Glushneva et al. (1983), Glushneva et al. (1998), and Kharitonov et al. (1997) obtained via the interface created by

⁴ The stars presented here were not included in *Gaia*’s DR1.

Mermilliod et al. (1997). The assigned uncertainties for the 2MASS infrared measurements are as reported in Cutri et al. (2003), and an uncertainty of 0.05 mag was assigned to the optical measurements.

We determined the best fit stellar spectral template to the photometry from the flux-calibrated stellar spectral atlas of Pickles (1998) using the χ^2 minimization technique (Press et al. 1992; Wall & Jenkins 2003). This gave us the bolometric flux (F_{BOL}) for each star and allowed for the calculation of extinction A_V with the wavelength-dependent reddening relations of Cardelli et al. (1989).

We combined our F_{BOL} values with the stars' distances to estimate L using $L = 4\pi d^2 F_{\text{BOL}}$. We also combined the F_{BOL} with θ_{LD} to determine each star's effective temperature by inverting the relation,

$$F_{\text{BOL}} = \frac{1}{4} \theta_{\text{LD}}^2 \sigma T_{\text{eff}}^4, \quad (2)$$

where σ is the Stefan-Boltzmann constant and θ_{LD} is in radians (van Belle et al. 1999). We follow Heiter et al. (2015), who established a systematic uncertainty of 5% on their F_{BOL} determinations from a sample of 34 benchmark *Gaia* stars. We therefore assigned an error of 5% for stars whose SED fits produced errors for F_{BOL} less than 5%. The resulting R , F_{BOL} , A_V , L , and T_{eff} are listed in Table 5.

Because μ_λ is chosen based on a given T_{eff} , we checked to see if μ_λ and therefore θ_{LD} would change based on our new T_{eff} . In most cases, μ_λ changed by an average of 0.01, and the largest difference was 0.11. The resulting θ_{LD} values changed at most by 1.5%, and the average difference was 0.2% (0.010 mas). This was well within the uncertainties on θ_{LD} , and re-calculating T_{eff} with the new θ_{LD} made at most a 47 K difference, which was for the hottest star in the sample (HD 120315, a 0.3% change), while the average difference was 8 K. These diameters and temperatures all converged after this one iteration, and these are the final values listed in Table 5.

3.3. Stellar Mass and Age

To estimate masses and ages for the evolved stars, we used the PARAM stellar model⁵ from Girardi et al. (2000) with a modified version of the method described in da Silva et al. (2006) and PARSEC isochrones from Bressan et al. (2012). For each star, the input parameters were its interferometrically determined T_{eff} , its [Fe/H] from the literature, its V magnitude from Mermilliod (1991), and its *Hipparcos* parallax from van Leeuwen (2007). The model used these inputs to derive each star's age, mass, radius, $(B - V)_0$, and $\log g$ using the isochrones and a Bayesian estimating method, calculating the probability density function separately for each property in question. da Silva et al. (2006) qualify mass estimates as “more uncertain” than other properties, so the resulting masses listed in Table 6 should be viewed as estimates only.

4. DISCUSSION

Several factors can affect a star's visibilities and subsequent angular diameter measurement: variability, binarity, or rapid rotation. None of the stars in our sample are variable to a degree that would be detectable in NPOI data. While some of the stars presented here do have binary companions, we could disregard the secondary star in our angular diameter fits to the primary star due to the separation between the components and/or the magnitude difference between them. Hutter et al. (2016)

⁵ http://stev.oapd.inaf.it/cgi-bin/param_1.0

recently demonstrated that the NPOI's detection sensitivity spans 3 to 860 mas with a magnitude difference of 3.0 (for most binary systems) to 3.5 (where the component spectral types differ by less than two). Any companions to our targets were beyond those detection limits.

Three of the stars are rapid rotators with $v \sin i$ higher than 100 km s⁻¹: HD 87901 (α Leo, Regulus), HD 159561 (α Oph, Rasalhague), and HD 187642 (α Lyr, Vega). The oblateness for these stars have been measured previously using the CHARA Array for Regulus (McAlister et al. 2005) and Rasalhague (Zhao et al. 2009), and the NPOI for Vega (Peterson et al. 2006). We do not directly measure the oblateness of these stars here, since the sampling of the $u - v$ plane for these stars do not give us enough coverage to detect asymmetries.

The size of the data set means we can use it to characterize the NPOI's performance. Figure 3 shows the percent error in θ_{LD} (σ_{LD}) versus θ_{LD} . The increase in errors as the diameter approaches 1 mas is expected, considering the resolution limit of the NPOI with the configurations used is ~ 1 mas. Above 3.5 mas, the errors are uniformly $\sim 1\%$ or smaller. As the NPOI gets the longer baselines as planned, the limiting resolution will get smaller and the associated errors will decrease. Eighty stars have $\sigma_{\text{LD}} \leq 2\%$, which is generally agreed to be the minimal standard of astrophysically useful stellar angular diameter measurements (Booth 1997; Holmberg et al. 2009). Note that one point is left off for the sake of clarity: HD 120315 with a diameter of 0.981 mas and an uncertainty of $\sim 15\%$.

Thirty-six of the 87 stars presented here do not have previously published interferometric angular diameters (see Table 7). Figure 4 shows the comparison between the diameters for those stars with published values and our measurements. The match is generally good, with some spread towards the smaller angular diameters that approach the resolution limits of some interferometers. Some of the variations between previous measurements and those presented here may be due to what limb-darkening law was used in the different studies.

The next step for these stars is to directly measure limb-darkening. Many of the stars presented here have data to or through and beyond the first null, where V^2 drops to zero. Before the first null, the visibility curve is dominated by the star's angular diameter. After the first null, second order effects such as limb-darkening become important, and specific limb-darkening models and prescriptions can be directly tested (Wittkowski et al. 2001). By verifying which limb-darkening models work the best for most stars, we will know how to characterize stars that are not observable using interferometry.

5. SUMMARY

We measured the angular diameters of 87 stars using the NPOI and found good agreement between our measurements and previous measurements when the latter were available. We combined our data with information from the literature to also determine the stars' temperatures, radii, bolometric fluxes, and luminosities. Finally we used the PARAM stellar model to estimate their masses and ages. These diameters will be of special interest when *Gaia* parallaxes are released with smaller errors than *Hipparcos* parallaxes, since that will allow us to more precisely measure the stars' physical radii and act as even stricter checks on stellar evolution and structure models.

We thank Brian Mason and William Hartkopf of the U.S. Naval Observatory, Washington, DC for their generosity with regard to data in the NPOI archive. The Navy Precision Optical Interferometer is a joint project of the Naval Research Laboratory and the U.S. Naval Observatory, in cooperation with Lowell Observatory, and is funded by the Office of Naval Research and the Oceanographer of the Navy. This research has made use of the SIMBAD database, operated at CDS, Strasbourg, France.

This publication makes use of data products from the Two Micron All Sky Survey, which is a joint project of the University of Massachusetts and the Infrared Processing and Analysis Center/California Institute of Technology, funded by the National Aeronautics and Space Administration and the National Science Foundation. This research has made use of the Jean-Marie Mariotti Center JSDC catalogue, available at http://www.jmmc.fr/catalogue_jsdc.htm.

REFERENCES

- Absil, O., di Folco, E., Mérand, A., et al. 2006, *A&A*, 452, 237
- Allende Prieto, C., & Lambert, D. L. 1999, *A&A*, 352, 555
- Alonso, A., Arribas, S., & Martinez-Roger, C. 1996, *A&AS*, 117, 227
- Anderson, E., & Francis, C. 2012, *Astronomy Letters*, 38, 331
- Armstrong, J. T., Mozurkewich, D., Rickard, L. J., et al. 1998, *ApJ*, 496, 550
- Armstrong, J. T., Nordgren, T. E., Germain, M. E., et al. 2001, *AJ*, 121, 476
- Aufdenberg, J. P., Mérand, A., Coudé du Foresto, V., et al. 2006, *ApJ*, 645, 664
- Baines, E. K., Armstrong, J. T., Schmitt, H. R., et al. 2014, *ApJ*, 781, 90
- Baines, E. K., Döllinger, M. P., Cusano, F., et al. 2010, *ApJ*, 710, 1365
- Baines, E. K., Döllinger, M. P., Guenther, E. W., et al. 2016, *AJ*, 152, 66
- Baines, E. K., McAlister, H. A., ten Brummelaar, T. A., et al. 2008, *ApJ*, 680, 728-733
- Baines, E. K., McAlister, H. A., ten Brummelaar, T. A., et al. 2009, *ApJ*, 701, 154
- Baines, E. K., McAlister, H. A., ten Brummelaar, T. A., et al. 2011, *ApJ*, 743, 130
- Baines, E. K., White, R. J., Huber, D., et al. 2012, *ApJ*, 761, 57
- Bazot, M., Ireland, M. J., Huber, D., et al. 2011, *A&A*, 526, L4
- Benson, J. A., Hummel, C. A., & Mozurkewich, D. 2003, Proc. SPIE, 4838, 358
- Berghofer, T. W., Schmitt, J. H. M. M., & Cassinelli, J. P. 1996, *A&AS*, 118, 481
- Booth, A. J. 1997, IAU Symposium, 189, 147
- Bordé, P., Coudé du Foresto, V., Chagnon, G., & Perrin, G. 2002, *A&A*, 393, 183
- Boyajian, T. S., McAlister, H. A., Cantrell, J. R., et al. 2009, *ApJ*, 691, 1243
- Boyajian, T. S., McAlister, H. A., van Belle, G., et al. 2012a, *ApJ*, 746, 101
- Boyajian, T., von Braun, K., Feiden, G. A., et al. 2015, *MNRAS*, 447, 846
- Boyajian, T. S., von Braun, K., van Belle, G., et al. 2012b, *ApJ*, 757, 112
- Boyajian, T. S., von Braun, K., van Belle, G., et al. 2013, *ApJ*, 771, 40
- Bressan, A., Marigo, P., Girardi, L., et al. 2012, *MNRAS*, 427, 127
- Cardelli, J. A., Clayton, G. C., & Mathis, J. S. 1989, *ApJ*, 345, 245
- Castelli, F., & Kurucz, R. L. 2004, arXiv:astro-ph/0405087
- Che, X., Monnier, J. D., Zhao, M., et al. 2011, *ApJ*, 732, 68
- Chelli, A., Duvert, G., Bourgès, L., et al. 2016, *A&A*, 589, A112
- Chiavassa, A., Norris, R., Montargès, M., et al. 2017, *A&A*, 600, L2
- Ciardi, D. R., van Belle, G. T., Akeson, R. L., et al. 2001, *ApJ*, 559, 1147
- Claret, A., & Bloemen, S. 2011, *A&A*, 529, A75
- Clem, J. L., Vandenberg, D. A., Grundahl, F., & Bell, R. A. 2004, *AJ*, 127, 1227
- Cohen, M., Wheaton, W. A., & Megeath, S. T. 2003, *AJ*, 126, 1090
- Colina, L., Bohlin, R. C., & Castelli, F. 1996, *AJ*, 112, 307
- Cox, A. N. 2000, *Allen's Astrophysical Quantities* (Melville, NY: AIP Press)
- Cutri, R. M., et al. 2003, The IRSA 2MASS All-Sky Point Source Catalog, NASA/IPAC Infrared Science Archive
- da Silva, L., Girardi, L., Pasquini, L., et al. 2006, *A&A*, 458, 609
- di Benedetto, G. P., & Rabbia, Y. 1987, *A&A*, 188, 114
- Domiciano de Souza, A., Kervella, P., Jankov, S., et al. 2005, *A&A*, 442, 567
- Duvert, G., Young, J., & Hummel, C. A. 2017, *A&A*, 597, A8

- Dyck, H. M., van Belle, G. T., & Thompson, R. R. 1998, AJ, 116, 981
- Eggen, O. J. 1968, Three-Colour Photometry of 4000 Northern Stars, London, H.M.S.O.
- Friedemann, C. 1992, Bulletin d'Information du Centre de Donnees Stellaires, 40, 31
- Gezari, D. Y., Schmitz, M., Pitts, P. S., & Mead, J. M. 1993, Catalog of Infrared Observations, NASA Reference Publication 1294 (3rd ed.; Greenbelt, MD: NASA)
- Girardi, L., Bressan, A., Bertelli, G., & Chiosi, C. 2000, A&AS, 141, 371
- Giridhar, S., Goswami, A., Kunder, A., Muneer, S., & Selvakumar, G. 2013, A&A, 556, A121
- Glushneva, I. N., Doroshenko, V. T., Fetisova, T. S., et al. 1983, Trudy Gosudarstvennogo Astronomicheskogo Instituta, 53, 50
- Glushneva, I. N., Doroshenko, V. T., Fetisova, T. S., et al. 1998, VizieR Online Data Catalog, 3207, 0
- Golay, M. 1972, Vistas in Astronomy, 14, 13
- Gray, R. O., Corbally, C. J., Garrison, R. F., McFadden, M. T., & Robinson, P. E. 2003, AJ, 126, 2048
- Gray, R. O., Napier, M. G., & Winkler, L. I. 2001, AJ, 121, 2148
- Häggkvist, L., & Oja, T. 1970, A&AS, 1, 199
- Hanbury Brown, R. H. 1968, ARA&A, 6, 13
- Hanbury Brown, R., Davis, J., & Allen, L. R. 1974a, MNRAS, 167, 121
- Hanbury Brown, R., Davis, J., Allen, L. R., & Rome, J. M. 1967, MNRAS, 137, 393
- Hanbury Brown, R., Davis, J., Lake, R. J. W., & Thompson, R. J. 1974b, MNRAS, 167, 475
- Heiter, U., Jofré, P., Gustafsson, B., et al. 2015, A&A, 582, A49
- Hekker, S., & Meléndez, J. 2007, A&A, 475, 1003
- Hohle, M. M., Neuhauser, R., & Schutz, B. F. 2010, Astronomische Nachrichten, 331, 349
- Holmberg, J., Nordström, B., & Andersen, J. 2009, A&A, 501, 941
- Houdashelt, M. L., Bell, R. A., & Sweigart, A. V. 2000, AJ, 119, 1448
- Huang, W., Gies, D. R., & McSwain, M. V. 2010, ApJ, 722, 605
- Huang, Y., Liu, X.-W., Yuan, H.-B., et al. 2015, MNRAS, 454, 2863
- Huber, D., Ireland, M. J., Bedding, T. R., et al. 2012, ApJ, 760, 32
- Hummel, C. A., Benson, J. A., Hutter, D. J., et al. 2003, AJ, 125, 2630
- Hutter, D. J., & Elias, N. M. II 2003, Proc. SPIE, 4838, 1234
- Hutter, D. J., Zavala, R. T., Tycner, C., et al. 2016, ApJS, 227, 4
- Jamar, C., Macau-Hercot, D., Monfils, A., et al. 1995, VizieR Online Data Catalog, 3039
- Jasevicius, V., Kuriliene, G., Strazdaite, V., et al. 1990, Vilnius Astronomijos Observatorijos Biuletinis, 85, 50
- Johnson, H. L., Mitchell, R. I., Iriarte, B., & Wisniewski, W. Z. 1966, Communications of the Lunar and Planetary Laboratory, 4, 99
- Jones, J., White, R. J., Quinn, S., et al. 2016, ApJL, 822, L3
- Katz, D., Soubiran, C., Cayrel, R., et al. 2011, A&A, 525, A90
- Kervella, P., Bigot, L., Gallenne, A., & Thévenin, F. 2017, A&A, 597, A137
- Kharitonov, A. V., Tereshchenko, V. M., & Knyazeva, L. N. 1997, VizieR Online Data Catalog, 3202, 0
- Koleva, M., & Vazdekis, A. 2012, A&A, 538, A143
- Kornilov, V. G., Volkov, I. M., Zakharov, A. I., et al. 1991, Trudy Gosudarstvennogo Astronomicheskogo Instituta, 63, 1
- Kovtyukh, V. V., Soubiran, C., Luck, R. E., et al. 2008, MNRAS, 389, 1336
- Lafrasse, S., Mella, G., Bonneau, D., et al. 2010, Proc. SPIE, 7734, 77344E-77344E-11
- Lane, B. F., Creech-Eakman, M. J., & Nordgren, T. E. 2002, ApJ, 573, 330
- Le Borgne, J.-F., Bruzual, G., Pelló, R., et al. 2003, A&A, 402, 433
- Ligi, R., Creevey, O., Mourard, D., et al. 2016, A&A, 586, A94
- Ligi, R., Mourard, D., Lagrange, A. M., et al. 2012, A&A, 545, A5
- Lindgren, L., Lammers, U., Hobbs, D., et al. 2012, A&A, 538, A78
- Ljunggren, B., & Oja, T. 1965, Arkiv for Astronomi, 3, 439
- McAlister, H. A., ten Brummelaar, T. A., Gies, D. R., et al. 2005, ApJ, 628, 439
- McClure, R. D., & Forrester, W. T. 1981, Publications of the Dominion Astrophysical Observatory Victoria, 15, 439

- Mermilliod, J. C. 1991, *Catalogue of Homogeneous Means in the UVB System*, Institut d'Astronomie, Universite de Lausanne
- Mermilliod, J.-C., Mermilliod, M., & Hauck, B. 1997, A&AS, 124, 349
- Milone, A. D. C., Sansom, A. E., & Sánchez-Blázquez, P. 2011, MNRAS, 414, 1227
- Monet, D. G., Levine, S. E., Canzian, B., et al. 2003, AJ, 125, 984
- Monnier, J. D., Che, X., Zhao, M., et al. 2012, ApJL, 761, L3
- Monnier, J. D., Townsend, R. H. D., Che, X., et al. 2010, ApJ, 725, 1192
- Monnier, J. D., Zhao, M., Pedretti, E., et al. 2007, Science, 317, 342
- Mourard, D., Clausse, J. M., Marcotto, A., et al. 2009, A&A, 508, 1073
- Mourard, D., Harmanec, P., Stencel, R., et al. 2012, A&A, 544, A91
- Mozurkewich, D., Armstrong, J. T., Hindsley, R. B., et al. 2003, AJ, 126, 2502
- Mozurkewich, D., Johnston, K. J., Simon, R. S., et al. 1991, AJ, 101, 2207
- Neckel, T., Klare, G., & Sarcander, M. 1980, Bulletin d'Information du Centre de Donnees Stellaires, 19, 61
- Nordgren, T. E., Germain, M. E., Benson, J. A., et al. 1999, AJ, 118, 3032
- Nordgren, T. E., Sudol, J. J., & Mozurkewich, D. 2001, AJ, 122, 2707
- Ohishi, N., Nordgren, T. E., & Hutter, D. J. 2004, ApJ, 612, 463
- Olsen, E. H. 1993, A&AS, 102, 89
- Otte, B., & Dixon, W. V. D. 2006, ApJ, 647, 312
- Peterson, D. M., Hummel, C. A., Pauls, T. A., et al. 2006, ApJ, 636, 1087
- Peterson, D. M., Hummel, C. A., Pauls, T. A., et al. 2006, Nature, 440, 896
- Pickles, A. J. 1998, PASP, 110, 863
- Press, W. H., Teukolsky, S. A., Vetterling, W. T., & Flannery, B. P. 1992, Numerical recipes in C. The art of scientific computing (Cambridge: University Press, c1992, 2nd ed.)
- Prugniel, P., Soubiran, C., Koleva, M., & Le Borgne, D. 2007, arXiv:astro-ph/0703658
- Prugniel, P., Vauglin, I., & Koleva, M. 2011, A&A, 531, A165
- Ramírez, I., & Meléndez, J. 2005, ApJ, 626, 446
- Reffert, S., Bergmann, C., Quirrenbach, A., Trifonov, T., & Künstler, A. 2015, A&A, 574, A116
- Richichi, A., Percheron, I., & Davis, J. 2009, MNRAS, 399, 399
- Sánchez-Blázquez, P., Peletier, R. F., Jiménez-Vicente, J., et al. 2006, MNRAS, 371, 703
- Savage, B. D., Massa, D., Meade, M., & Wesselius, P. R. 1985, ApJS, 59, 397
- Shao, M., & Colavita, M. M. 1992, ARA&A, 30, 457
- Shao, M., Colavita, M. M., Hines, B. E., et al. 1988, ApJ, 327, 905
- Soubiran, C., Le Campion, J.-F., Brouillet, N., & Chemin, L. 2016, A&A, 591, A118
- Stencel, R. E., Creech-Eakman, M., Hart, A., et al. 2008, ApJL, 689, L137
- Tycner, C., Hutter, D. J., & Zavala, R. T. 2010, Proc. SPIE, 7734, 103T
- Valdes, F., Gupta, R., Rose, J. A., Singh, H. P., & Bell, D. J. 2004, ApJS, 152, 251
- Valentini, M., & Munari, U. 2010, A&A, 522, A79
- van Belle, G. T., Ciardi, D. R., Thompson, R. R., Akeson, R. L., & Lada, E. A. 2001, ApJ, 559, 1155
- van Belle, G. T., Lane, B. F., Thompson, R. R., et al. 1999, AJ, 117, 521
- van Belle, G. T., Paladini, C., Aringer, B., Hron, J., & Ciardi, D. 2013, ApJ, 775, 45
- van Belle, G. T., van Belle, G., Creech-Eakman, M. J., et al. 2008, ApJS, 176, 276-292
- van Belle, G. T., Creech-Eakman, M. J., & Hart, A. 2009, MNRAS, 394, 1925
- van Belle, G. T., & von Braun, K. 2009, ApJ, 694, 1085
- van Leeuwen, F. 2007, A&A, 474, 653
- Wall, J. V., & Jenkins, C. R. 2003, Practical Statistics for Astronomers, Cambridge Observing Handbooks for Research Astronomers, vol. 3. (Cambridge, UK: Cambridge University Press)
- Wittkowski, M., Hummel, C. A., Johnston, K. J., et al. 2001, A&A, 377, 981
- Wittkowski, M., Chiavassa, A., Freytag, B., et al. 2016, A&A, 587, A12
- Wittkowski, M., Arroyo-Torres, B., Marcaide, J. M., et al. 2017, A&A, 597, A9
- Wu, Y., Singh, H. P., Prugniel, P., Gupta, R., & Koleva, M. 2011, A&A, 525, A71

- Zhao, M., Monnier, J. D., Pedretti, E., et al. 2009,
ApJ, 701, 209
- Zorec, J., Cidale, L., Arias, M. L., et al. 2009,
A&A, 501, 297

Table 1. Sample Star Properties.

HD	HR	FK5	Other	Spectral	V	Parallax		
			Name	Type	(mag)	(mas)	[Fe/H]	Ref
432	21	2	β Cas	F2 III	2.27±0.01	59.58±0.38	0.03	1
1013	45	1004	χ Peg	M2 III	4.80±0.01	8.86±0.22	0.00	2
1522	74	9	ι Cet	K1 III	3.54±0.02	11.88±0.18	0.08	1
8512	402	47	θ Cet	K0 III	3.60±0.01	28.66±0.19	-0.07	1
9927	464	52	v Per	K3 III	3.57±0.01	18.41±0.18	0.07	3
17709	843	2198	17 Per	K5.5 III	4.54±0.01	6.98±0.44	-0.26	1
18925	915	108	γ Per	G9 III	2.93±0.01	13.41±0.51	-0.10	1
20644	999	2234	-	K3 III	4.47±0.01	6.01±0.25	-0.27	1
28305	1409	164	ϵ Tau	G9.5 III	3.54±0.01	22.24±0.25	0.14	1
31964	1605	183	ϵ Aur	A9 I	2.98±0.02	1.53±1.29	-0.11	4
34085	1713	194	β Ori	B8 I	0.14±0.03	3.78±0.34	0.00	2
38944	2011	2440	v Aur	M0 III	4.74±0.01	6.24±0.65	0.00	2
43232	2227	2475	γ Mon	K1 III	3.97±0.01	6.55±0.19	-0.13	1
48329	2473	254	ϵ Gem	G8 I	2.99±0.01	3.86±0.17	0.11	1
58207	2821	282	ι Gem	G9 III	3.79±0.01	27.10±0.20	-0.10	1
62345	2985	294	κ Gem	G8 III	3.57±0.01	23.07±0.22	0.02	1
62509	2990	295	β Gem	K0 III	1.14±0.01	96.54±0.27	0.08	1
66141	3145	2623	-	K2 III	4.39±0.01	12.84±0.25	-0.26	1
69267	3249	312	β Cnc	K4 III	3.53±0.01	10.75±0.19	-0.17	1
70272	3275	314	31 Lyn	K4 III	4.25±0.01	8.53±0.25	-0.06	1
76294	3547	334	ζ Hya	G8.5 III	3.11±0.01	19.51±0.18	-0.08	1
82308	3773	2756	λ Leo	K4.5 III	4.31±0.01	9.91±0.18	-0.21	1
82328	3775	358	θ UMa	F7 V	3.18±0.01	74.19±0.14	-0.16	1
83618	3845	1250	ι Hya	K2.5 III	3.90±0.01	12.39±0.14	-0.09	1
84441	3873	367	ϵ Leo	G1 III	2.98±0.01	13.22±0.15	-0.09	1
85503	3905	371	μ Leo	K2 III	3.88±0.01	26.28±0.16	0.25	1
87901	3982	380	α Leo	B8 IV	1.36±0.01	41.13±0.35	0.21	1
94264	4247	412	46 LMi	K0 III-IV	3.82±0.02	34.38±0.21	-0.07	1
95689	4301	417	α UMa	G9 III	1.80±0.01	26.54±0.48	-0.15	1
96833	4335	420	ψ UMa	K1 III	3.01±0.01	22.57±0.14	-0.06	1
97778	4362	2897	72 Leo	M3 II	4.63±0.01	3.40±0.65	-0.03	5
98262	4377	425	ν UMa	K3 III	3.48±0.01	8.17±0.17	-0.11	1
100029	4434	433	λ Dra	M0 III	3.85±0.02	9.79±0.15	0.00	2
102212	4517	1302	ν Vir	M1 III	4.03±0.01	11.10±0.18	-0.41	1
108381	4737	2999	γ Com	K1 III	4.35±0.01	19.50±0.19	0.19	1
108907	4765	-	4 Dra	M3 III	4.96±0.01	5.25±0.48	0.00	2
109358	4785	470	β CVn	G0 V	4.26±0.01	118.49±0.20	-0.19	1
113226	4932	488	ϵ Vir	G8 III	2.83±0.02	29.76±0.14	0.13	1

Table 1 continued on next page

Table 1 (*continued*)

HD	HR	FK5	Other	Name	Spectral	V	Parallax		
					Type	(mag)	(mas)	[Fe/H]	Ref
113996	4954	3045	41 Com	K5 III	4.80±0.02	9.84±0.22	-0.09	1	
117675	5095	3079	74 Vir	M2.5 III	4.69±0.01	8.16±0.19	0.00	2	
120136	5185	507	τ Boo	F6 IV	4.50±0.01	64.03±0.19	0.24	1	
120315	5191	509	η UMa	B3 V	1.86±0.01	31.38±0.24	-0.14	1	
120477	5200	-	v Boo	K5.5 III	4.05±0.02	12.38±0.23	-0.28	1	
120933	5219	3102	-	M3 III	4.75±0.02	5.43±0.20	0.12	1	
121130	5226	511	i Dra	M3.5 III	4.66±0.02	8.78±0.20	-0.24	1	
127665	5429	534	ρ Boo	K3 III	3.58±0.01	20.37±0.18	-0.08	1	
129712	5490	1383	34 Boo	M3 III	4.81±0.01	4.63±0.28	0.00	2	
133124	5600	3185	ω Boo	K4 III	4.82±0.01	8.78±0.28	0.05	1	
133208	5602	555	β Boo	G8 III	3.51±0.03	14.48±0.14	0.03	1	
136726	5714	-	11 UMi	K4 III	5.01±0.01	8.19±0.19	0.05	1	
137759	5744	571	ι Dra	K2 III	3.29±0.02	32.23±0.10	0.09	1	
140573	5854	582	α Ser	K2 III	2.64±0.01	44.10±0.19	0.13	1	
143107	5947	593	ϵ CrB	K2 III	4.14±0.01	14.73±0.21	-0.20	1	
148387	6132	-	η Dra	G8 III	2.73±0.01	35.42±0.09	-0.07	1	
148856	6148	618	β Her	G7 III	2.78±0.02	23.44±0.58	-0.21	1	
150997	6220	626	η Her	G7 III	3.50±0.03	30.02±0.11	-0.22	1	
156283	6418	643	π Her	K3 II	3.16±0.02	8.66±0.12	-0.04	1	
159561	6556	656	α Oph	A5 III	2.08±0.01	67.13±1.06	-0.16	1	
161096	6603	665	β Oph	K2 III	2.77±0.01	39.85±0.17	0.14	1	
161797	6623	667	μ Her	G5 IV	3.42±0.01	120.33±0.16	0.23	1	
163917	6698	673	ν Oph	G9 III	3.34±0.01	21.64±0.26	0.12	1	
169414	6895	690	109 Her	K2 III	3.83±0.01	27.42±0.40	-0.06	1	
170693	6945	3465	42 Dra	K1.5 III	4.83±0.02	10.36±0.20	-0.49	1	
172167	7001	699	α Lyr	A0 V	0.03±0.01	130.23±0.36	-0.56	1	
176524	7180	714	v Dra	K0 III	4.83±0.03	9.48±0.45	-0.03	1	
176678	7193	-	i Aql	K1 III	4.02±0.01	22.66±0.23	-0.04	1	
180610	7309	-	54 Dra	K2 III	4.98±0.01	19.74±0.18	0.07	1	
181276	7328	726	κ Cyg	G9 III	3.79±0.02	26.27±0.10	0.04	1	
183439	7405	1508	α Vul	M0.5 III	4.44±0.02	10.97±0.28	-0.38	1	
186791	7525	741	γ Aql	K3 II	2.72±0.01	8.26±0.17	-0.20	1	
187642	7557	745	α Aql	A7 V	0.77±0.02	194.95±0.57	-0.24	1	
187929	7570	746	η Aql	F6 I	3.73±0.14	2.36±1.04	0.13	1	
188310	7595	-	ξ Aql	G9.5 III	4.70±0.02	17.77±0.29	-0.23	1	
196094	7866	-	47 Cyg	K6 I	4.61±0.02	1.18±0.41	0.13	6	
203504	8173	804	1 Peg	K1 III	4.09±0.01	20.93±0.17	-0.01	1	
204867	8232	808	β Aqr	G0 I	2.90±0.02	6.07±0.22	0.01	1	
206952	8317	817	11 Cep	K0.5 III	4.56±0.01	17.88±0.40	0.17	1	
209750	8414	827	α Aqr	G2 I	2.94±0.02	6.23±0.19	0.16	1	

Table 1 continued on next page

Table 1 (*continued*)

HD	HR	FK5	Other	Spectral	V	Parallax		
				Name	Type	(mag)	(mas)	[Fe/H]
211388	8498	-	1 Lac	K3 II-III	4.14±0.02	5.25±0.23	-0.01	1
212496	8538	844	β Lac	G9 III	4.44±0.01	19.19±0.16	-0.40	1
213311	8572	3799	5 Lac	K9 I	4.37±0.01	1.98±0.18	0.00	2
215182	8650	857	η Peg	G8 II	2.95±0.01	15.22±0.71	-0.13	1
218329	8795	1603	55 Peg	M1 III	4.53±0.02	9.92±0.29	0.23	5
219215	8834	1607	φ Aqr	M1.5 III	4.22±0.01	16.14±0.89	0.00	2
219449	8841	1608	91 Aqr	K1 III	4.23±0.01	21.77±0.29	0.00	1
219615	8852	878	γ Psc	G9 III	3.70±0.01	23.64±0.18	-0.49	1
222404	8974	893	γ Cep	K1III-IV	3.21±0.01	70.91±0.40	0.15	1

NOTE—Spectral types are from *SIMBAD*, *V* magnitudes are from [Mermilliod \(1991\)](#), parallaxes are from [van Leeuwen \(2007\)](#), and [Fe/H] are from the following sources: 1. [Anderson & Francis \(2012\)](#); 2. no [Fe/H] was available so 0.00 was used; 3. [Reffert et al. \(2015\)](#); 4. [Giridhar et al. \(2013\)](#); 5. [Katz et al. \(2011\)](#) and 6. [Soubiran et al. \(2016\)](#).

Table 2. Observing Log.

Target HD	Calibrator HD	Date (UT)	Baselines Used [†]	#
				Obs
432	3360	2005 Sep 29	AW-E6	150
		2005 Sep 30	AC-AE, AC-AN, AC-AW, AC-E6, AE-AN, AW-E6	600
		2005 Oct 3	AC-AN, AE-AN	80
		2005 Oct 6	AC-AW, AC-E6, AW-E6	120
		2005 Oct 7	AC-AN, AC-E6, AE-AN, AW-E6	360
		2005 Oct 8	AW-E6	89
		2005 Oct 11	AW-E6	150
1013	886	2007 Oct 19	AC-AE, AC-AN, AC-AW, AE-AN	60
		2007 Oct 20	AC-AE, AC-E6, AE-AN, AW-E6	212
		2007 Nov 4	AC-AE, AC-AN, AC-AW, AE-AN	156
214923		2007 Oct 19	AC-AE, AW-E6	30
		2007 Oct 20	AC-AE, AC-E6, AE-AN, AW-E6	212
		2007 Nov 4	AC-AE, AC-AN, AC-AW, AE-AN	154
1522	222603	2010 Nov 19	AC-AE, AC-E6, AE-W7, E6-W7	189
		2010 Dec 8	AC-AE, AC-W7, AE-W7	29

NOTE—[†]The maximum baseline lengths are AC-AE 18.9 m, AC-AN 22.8 m, AC-AW 22.2 m, AC-E6 34.4 m, AC-W7 51.3 m, AE-AN 34.9 m, AE-W7 64.2 m, AW-E6 53.3 m, and E6-W7 79.4 m. This table shows the information for several stars as an example; the full table is available on the electronic version of the *Astronomical Journal*.

Table 3. Calibrator Stars' SED Inputs and Angular Diameters.

HD	Spec Type	Spec	<i>U</i>	<i>B</i>	<i>V</i>	<i>R</i>	<i>I</i>	<i>J</i>	<i>H</i>	<i>K</i>	T_{eff}	$\log g$		θ_{est}	
		(mag)	(mag)	(mag)	(mag)	(mag)	(mag)	(mag)	(mag)	(mag)	(K)	(cm s ⁻²)	Ref	<i>E(B - V)</i>	Ref
886	B2 IV	1.75	2.61	2.83	2.88	3.06	3.50	3.64	3.77	21944	3.93	1	0.02	11	0.45±0.02
2905	B1 I	3.50	4.30	4.16	4.12	4.09	4.14	4.15	4.01	22160	2.84	2,3	0.33	12	0.36±0.02
3360	B2 IV	2.62	3.47	3.66	3.74	3.92	4.14	4.25	4.25	20900	3.9	4	0.03	2	0.34±0.02
6658	A3	5.29	5.15	5.04	4.96	4.90	5.10	5.00	4.77	8511	4.04	5	0.00	N/A	0.37±0.02
11171	F0 V	5.04	5.00	4.67	4.47	4.31	3.66	3.47	3.87	7244	4.24	5	0.02	13	0.66±0.03
11415	B3 V	2.62	3.22	3.37	3.40	3.53	3.86	3.93	3.96	14250	3.38	6	0.05	14	0.50±0.03
17573	B8 V	3.16	3.51	3.61	3.64	3.73	3.66	3.80	3.86	11749	4.14	5	0.01	2	0.52±0.03
25642	A0 IV	4.23	4.27	4.29	4.27	4.30	4.08	4.15	4.15	9790	4.1	4	0.08	13	0.50±0.03
27819	A2 V	5.08	4.95	4.80	4.71	4.62	4.56	4.51	4.41	8318	4.11	5	0.05	11	0.47±0.02
27934	A7 IV-V	4.48	4.36	4.22	4.13	4.06	4.09	4.06	4.08	8128	3.80	5	0.05	13	0.61±0.03
32630	B3 V	2.33	2.99	3.17	3.21	3.35	3.61	3.76	3.86	14125	3.94	5	0.02	2	0.52±0.03
34503	B5 III	3.00	3.47	3.59	3.62	3.73	3.90	3.89	3.88	14000	3.4	4	0.05	2	0.46±0.02
45725	B4 V	3.87	4.50	4.60	4.69	4.82	3.72	3.52	4.08	21135	4.00	7	0.04	14	0.30±0.02
50019	A2 IV	3.84	3.70	3.60	3.53	3.48	3.25	3.23	3.16	8128	3.50	5	0.03	13	0.83±0.04
56537	A4 IV	3.79	3.69	3.58	3.50	3.44	3.54	3.50	3.54	8511	4.10	5	0.02	13	0.75±0.04
58946	F1 V	4.47	4.49	4.18	4.00	3.84	3.22	3.16	2.98	7244	4.26	5	0.00	15	0.83±0.04
71115	G6 III	6.71	6.07	5.13	4.59	4.13	3.61	3.07	2.92	4800	2.34	3	0.00	N/A	1.29±0.06
71155	A0 V	3.86	3.88	3.90	3.89	3.92	4.12	4.09	4.08	9772	4.16	5	0.03	2	0.54±0.03
74198	A1 IV	4.70	4.68	4.67	4.64	4.65	4.80	4.79	4.64	9550	4.19	5	0.00	13	0.38±0.02
76756	A7 V	4.58	4.40	4.26	4.18	4.11	3.98	4.03	3.94	7943	3.73	5	0.00	N/A	0.60±0.03
79469	B9.5 V	3.71	3.82	3.89	3.89	3.95	3.46	4.04	3.94	10715	4.23	5	0.00	16	0.51±0.03
87696	A7 V	4.74	4.67	4.49	4.38	4.29	4.27	4.05	4.00	7943	4.27	5	0.01	13	0.56±0.03
87737	A0 I	3.25	3.46	3.49	3.50	3.54	3.50	3.50	3.30	9650	1.95	7	0.00	11	0.65±0.03
89021	A1 IV	3.54	3.48	3.45	3.40	3.40	3.44	3.46	3.42	8913	3.84	5	0.01	2	0.74±0.04
90277	F0 V	5.16	4.99	4.74	4.59	4.46	4.55	4.26	3.97	7413	3.62	5	0.01	13	0.55±0.03
91312	A7 IV	5.05	4.97	4.75	4.61	4.50	4.12	4.06	4.20	7943	4.18	5	0.03	13	0.53±0.03
95128	G1 V	5.78	5.66	5.05	4.67	4.36	3.96	3.74	3.75	5860	4.31	7	0.00	11	0.79±0.04
95608	A1 V	4.53	4.48	4.42	4.37	4.35	4.32	4.32	4.32	9120	4.22	5	0.04	13	0.48±0.02

Table 3 continued on next page

Table 3 (*continued*)

HD	Spec Type	Spec	<i>U</i>	<i>B</i>	<i>V</i>	<i>R</i>	<i>I</i>	<i>J</i>	<i>H</i>	<i>K</i>	<i>T</i> _{eff}	<i>log g</i>		θ_{est}	
		(mag)	(mag)	(mag)	(mag)	(mag)	(mag)	(mag)	(mag)	(mag)	(K)	(cm s ⁻²)	Ref	<i>E(B - V)</i>	Ref
97633	A2 IV	3.37	3.33	3.34	3.29	3.30	3.12	3.19	3.08	9120	3.62	5	0.01	11	0.78±0.04
98664	B9.5 V	3.89	3.99	4.04	4.07	4.13	4.37	4.33	4.14	10233	3.89	5	0.02	2	0.48±0.02
103287	A0 V	2.45	2.44	2.44	2.36	2.35	2.38	2.49	2.43	9272	3.64	8	0.02	13	1.15±0.06
106591	A2 V	3.46	3.39	3.31	3.24	3.21	3.32	3.31	3.10	8710	4.12	5	0.00	13	0.81±0.04
108283	F0	5.39	5.21	4.95	4.78	4.65	4.41	4.24	4.15	7244	3.48	5	0.02	17	0.54±0.03
109387	B6 III	3.15	3.73	3.85	3.92	4.03	3.82	3.91	3.82	14380	3.15	1	0.02	14	0.44±0.02
112413	A0 V	2.45	2.78	2.89	2.88	2.94	3.06	3.13	3.15	12589	4.23	5	0.01	11	0.67±0.03
118098	A2 V	3.60	3.49	3.37	3.31	3.25	3.26	3.15	3.22	8511	4.19	5	0.00	18	0.81±0.04
120136	F6 IV	5.03	4.98	4.50	4.21	3.96	3.62	3.55	3.51	6457	4.25	5	0.00	19	0.82±0.04
122408	A3 V	4.48	4.36	4.25	4.19	4.14	4.21	4.11	4.09	8128	3.58	5	0.11	20	0.64±0.03
125162	A0 V	4.32	4.26	4.18	4.13	4.10	3.98	4.03	3.91	8710	4.26	5	0.01	21	0.56±0.03
128167	F4 V	4.75	4.83	4.47	4.27	4.10	3.56	3.46	3.34	6918	4.37	5	0.00	15	0.76±0.04
137422	A2 III	3.20	3.11	3.05	2.96	2.94	2.90	2.77	2.71	9300	2.09	3	0.02	2	0.87±0.04
141003	A2 IV	3.82	3.73	3.67	3.60	3.57	3.44	3.54	3.55	8511	3.69	5	0.02	2	0.73±0.04
141513	A0 V	3.42	3.50	3.54	3.56	3.60	3.80	3.76	3.70	9772	3.88	5	0.02	13	0.63±0.03
141795	A2	3.99	3.86	3.71	3.63	3.56	3.56	3.44	3.43	8318	4.26	5	0.00	22	0.72±0.04
147394	B5 IV	3.19	3.74	3.90	3.94	4.07	3.93	4.09	4.29	14791	3.98	5	0.03	2	0.38±0.02
147547	A9 III	4.21	4.02	3.75	3.58	3.44	3.27	3.12	2.94	7079	3.26	5	0.03	13	0.97±0.05
149212	A0 III	4.80	4.91	4.96	4.98	5.03	4.86	4.96	4.96	9980	3.4	4	0.02	23	0.33±0.02
156164	A1 IV	3.28	3.20	3.12	3.07	3.04	2.83	2.98	2.81	8710	4.06	5	0.00	13	0.91±0.05
160613	A2 V	4.42	4.33	4.25	4.18	4.15	4.25	4.18	4.11	8511	3.80	5	0.03	13	0.55±0.03
161868	A1 V	3.83	3.78	3.74	3.70	3.69	3.59	3.66	3.62	9120	4.20	5	0.05	13	0.67±0.03
166014	B9.5 III	3.77	3.81	3.84	3.85	3.89	3.97	3.96	3.95	10590	4.17	9	0.02	14	0.52±0.02
171635	F7 I	5.83	5.40	4.79	4.40	4.09	3.09	2.93	2.70	6130	1.52	10	0.05	24	0.96±0.05
176437	B9 III	3.10	3.20	3.25	3.24	3.28	3.12	3.23	3.12	10500	3.4	4	0.02	11	0.71±0.04
177724	A0 IV	3.01	3.00	2.99	2.94	2.94	3.08	3.05	2.88	9333	4.09	5	0.05	2	0.91±0.05
177756	B9 V	3.07	3.34	3.43	3.44	3.52	3.52	3.48	3.56	11749	4.22	5	0.00	15	0.56±0.03
182564	A0 III	4.67	4.61	4.59	4.56	4.56	4.55	4.58	4.45	8913	3.85	5	0.01	13	0.44±0.02
184006	A5 V	4.07	3.93	3.78	3.69	3.62	3.74	3.69	3.60	8180	4.29	3	0.00	13	0.70±0.04
187691	F8 V	5.75	5.67	5.12	4.81	4.54	4.23	3.86	3.90	6310	4.32	5	0.03	11	0.68±0.03

Table 3 continued on next page

Table 3 (*continued*)

HD	Spec Type	Spec	<i>U</i>	<i>B</i>	<i>V</i>	<i>R</i>	<i>I</i>	<i>J</i>	<i>H</i>	<i>K</i>	T_{eff}	$\log g$	Ref	$E(B - V)$	Ref	θ_{est}
			(mag)	(K)	(cm s ⁻²)											
192907	B9 III	4.22	4.33	4.38	4.43	4.49	4.51	4.42	4.43	10350	3.65	7	0.02	11	0.41±0.02	
195810	B6 III	3.44	3.91	4.03	4.07	4.18	4.66	4.55	4.38	13600	2.44	3	0.02	14	0.39±0.02	
197461	A7 IV-V	4.84	4.74	4.43	4.28	4.14	3.90	3.75	3.83	7244	3.48	5	0.00	25	0.66±0.03	
198001	B9.5 V	3.81	3.77	3.77	3.76	3.77	3.85	3.67	3.74	9120	3.55	5	0.02	11	0.63±0.03	
210418	A1 V	3.69	3.60	3.52	3.47	3.44	3.46	3.39	3.38	8511	4.02	5	0.03	2	0.78±0.04	
210459	F5 III	4.93	4.75	4.29	4.01	3.78	3.49	3.30	3.12	6457	3.09	5	0.00	25	0.90±0.05	
212061	A0 V	3.68	3.79	3.85	3.86	3.91	4.11	4.05	4.02	10471	4.11	5	0.02	2	0.52±0.03	
213558	A1 V	3.78	3.77	3.76	3.75	3.76	3.83	3.87	3.85	9333	4.20	5	0.00	15	0.60±0.03	
214923	B8 V	3.10	3.32	3.41	3.43	3.51	3.54	3.53	3.57	10965	3.75	5	0.01	2	0.60±0.03	
216627	A3 V	3.43	3.33	3.27	3.21	3.18	3.27	3.20	3.16	8511	3.58	5	0.02	13	0.86±0.04	
217891	B6 V	3.93	4.41	4.53	4.52	4.63	4.76	4.81	4.75	14000	4.0	4	0.03	14	0.29±0.01	
219688	B7 V	3.69	4.24	4.39	4.46	4.60	4.70	4.76	4.76	14125	4.13	5	0.02	14	0.30±0.02	
222603	A7 V	4.78	4.70	4.50	4.38	4.27	4.37	4.20	4.06	7943	4.21	5	0.00	20	0.54±0.03	

NOTE—Spectral types are from SIMBAD; *UBV* values are from Mermilliod (1991); *RI* values are from Monet et al. (2003); *JHK* values are from Cutri et al. (2003); T_{eff} , $\log g$, and $E(B - V)$ values are from the following sources: 1: Prugniel et al. (2007); 2: Zorec et al. (2009); 3: Cox (2000) based on SIMBAD spectral type; 4: Lafrasse et al. (2010); 5: Allende Prieto & Lambert (1999); 6: Huang et al. (2010); 7: Soubiran et al. (2016); 8: Gray et al. (2003); 9: Wu et al. (2011); 10: Gray et al. (2001); 11: Sánchez-Blázquez et al. (2006); 12: Savage et al. (1985); 13: Neckel et al. (1980); 14: Friedemann (1992); 15: Alonso et al. (1996); 16: Berghofer et al. (1996); 17: Valentini & Munari (2010); 18: Huang et al. (2015); 19: Ramírez & Meléndez (2005); 20: van Belle et al. (2008); 21: Otte & Dixon (2006); 22: Koleva & Vazdekis (2012); 23: Jamar et al. (1995); 24: Kovtyukh et al. (2008); 25: Clem et al. (2004). θ_{est} is the estimated angular diameter calculated using the method described in Section 2.

Table 4. Interferometric Results.

Target	θ_{UD}	T_{eff}	$\log g$	Ref	Initial	θ_{LD}	Final	θ_{LD}	σ_{LD}	Max SF
	HD	(mas)	(K)		μ_λ	(mas)	μ_λ	(mas)	(%)	(10 ⁶ cycles s ⁻¹)
432	2.032	6810	4.09	1	0.49	2.013±0.015	0.49	2.103±0.015	0.7	94.9
1013	4.041	3540	0.8	2	0.83	4.367±0.022	0.82	4.359±0.022	0.5	74.9
1522	3.380	4390	2.0	2	0.73	3.328±0.062	0.70	3.310±0.062	1.9	119.1
8512	2.625	4677	2.57	3	0.69	2.784±0.016	0.64	2.764±0.016	0.6	119.2
9927	3.389	4365	2.01	3	0.73	3.649±0.007	0.73	3.649±0.007	0.2	80.7
17709	3.648	4050	1.7	2	0.77	3.907±0.021	0.77	3.907±0.021	0.5	81.1
18925	3.651	5623	2.44	3	0.57	3.831±0.018	0.70	3.894±0.018	0.5	34.3
20644	3.476	4390	2.0	2	0.71	3.680±0.025	0.70	3.674±0.025	0.7	81.1
28305	2.439	4786	2.47	3	0.69	2.599±0.050	0.67	2.592±0.050	1.9	90.4
31964	2.129	7030	2.26	4	0.52	2.221±0.012	0.48	2.210±0.012	0.5	120.2
34085	2.526	11100	2.29	4	0.40	2.603±0.009	0.41	2.606±0.009	0.3	116.9
38944	4.055	3600	1.1	2	0.82	4.325±0.036	0.80	4.310±0.036	0.8	82.3
43232	2.958	4250	2.0	2	0.74	3.125±0.034	0.68	3.097±0.034	1.1	93.1
48329	4.468	4386	0.76	5	0.73	4.736±0.013	0.65	4.677±0.013	0.3	82.3
58207	2.262	4700	2.2	2	0.68	2.401±0.024	0.65	2.390±0.024	1.0	118.8
62345	2.226	4800	2.2	2	0.68	2.378±0.025	0.63	2.361±0.025	1.1	113.1
62509	7.570	4786	2.77	3	0.69	8.108±0.013	0.71	8.134±0.013	0.2	51.2
66141	2.558	4390	2.0	2	0.72	2.755±0.039	0.70	2.747±0.039	1.4	95.6
69267	4.784	4150	1.9	2	0.75	5.167±0.035	0.75	5.167±0.035	0.7	81.1
70272	3.974	4050	1.7	2	0.78	4.241±0.024	0.76	4.228±0.024	0.6	82.2
76294	2.988	4800	2.2	2	0.68	3.209±0.017	0.65	3.196±0.017	0.5	80.4
82308	3.909	4050	1.7	2	0.77	4.155±0.025	0.75	4.143±0.025	0.6	82.4
82328	1.598	6457	3.94	3	0.50	1.658±0.013	0.52	1.662±0.013	0.8	99.3
83618	3.236	4250	2.0	2	0.74	3.484±0.033	0.70	3.462±0.033	1.0	81.0
84441	2.469	5600	2.9	2	0.57	2.587±0.025	0.57	2.587±0.025	1.0	116.9
85503	2.693	4660	2.1	2	0.71	2.887±0.016	0.71	2.887±0.016	0.6	78.3
87901	1.626	10965	3.77	3	0.38	1.667±0.037	0.36	1.664±0.037	2.2	82.0
94264	2.460	4660	2.1	2	0.69	2.626±0.009	0.69	2.626±0.009	0.3	119.9
95689	6.352	4655	2.20	6	0.69	6.471±0.041	0.64	6.419±0.041	0.6	49.0

Table 4 continued on next page

Table 4 (*continued*)

Target	θ_{UD}	T_{eff}	$\log g$	Initial	θ_{LD}	Final	θ_{LD}	σ_{LD}	Max SF	
	HD	(mas)	(K)	(cm s ⁻²)	Ref	μ_λ	(mas)	μ_λ	(mas)	(%)
96833	3.890	4571	2.08	3	0.71	4.139±0.007	0.70	4.131±0.007	0.2	81.2
97778	5.721	3734	1.16	7	0.82	6.182±0.057	0.82	6.182±0.057	0.9	53.5
98262	4.282	4250	2.0	2	0.74	4.568±0.016	0.73	4.561±0.016	0.4	81.4
100029	5.852	3690	1.3	2	0.82	6.376±0.012	0.82	6.376±0.012	0.2	47.4
102212	5.212	3690	1.3	2	0.81	5.657±0.013	0.81	5.657±0.013	0.2	53.2
108381	2.034	4571	2.39	3	0.72	2.185±0.057	0.70	2.179±0.057	2.6	33.5
108907	4.959	3630	1.24	4	0.82	5.420±0.010	0.82	5.420±0.010	0.2	57.1
109358	1.077	5888	4.37	3	0.55	1.134±0.019	0.54	1.133±0.034	3.0	82.4
113226	3.170	5012	2.67	3	0.65	3.318±0.013	0.65	3.318±0.013	0.4	81.2
113996	2.863	4050	1.7	2	0.77	3.104±0.019	0.74	3.090±0.019	0.6	79.1
117675	5.102	3500	0.6	2	0.84	5.951±0.049	0.84	5.951±0.049	0.8	81.1
120136	0.783	6457	4.25	3	0.52	0.822±0.038	0.52	0.822±0.049	6.0	99.3
120315	0.937	11220	3.78	3	0.37	0.987±0.144	0.30	0.981±0.144	14.7	52.9
120477	4.372	4050	1.7	2	0.76	4.691±0.022	0.76	4.691±0.022	0.5	67.7
120933	5.460	3820	1.52	8	0.80	5.922±0.042	0.81	5.932±0.042	0.7	52.9
121130	6.161	3652	1.00	9	0.82	6.788±0.077	0.83	6.799±0.077	1.1	42.9
127665	3.663	4266	2.04	3	0.74	3.901±0.008	0.74	3.901±0.008	0.2	81.1
129712	5.119	3500	1.24	4	0.82	5.573±0.055	0.82	5.573±0.055	1.0	52.5
133124	2.821	4150	1.9	2	0.76	3.055±0.077	0.76	3.055±0.077	2.5	57.2
133208	2.359	4800	2.2	2	0.68	2.495±0.008	0.65	2.484±0.008	0.3	120.4
136726	2.018	4120	2.03	8	0.76	2.156±0.023	0.74	2.149±0.023	1.1	120.2
137759	3.367	4466	2.24	3	0.71	3.576±0.011	0.68	3.559±0.011	0.3	81.2
140573	4.521	4467	2.24	3	0.71	4.755±0.013	0.70	4.770±0.013	0.3	81.1
143107	2.780	4250	2.0	2	0.73	3.001±0.128	0.72	2.997±0.128	4.3	45.1
148387	3.261	5012	2.74	3	0.65	3.470±0.010	0.65	3.470±0.010	0.3	81.2
148856	3.280	5012	2.47	3	0.64	3.472±0.008	0.64	3.472±0.008	0.2	81.2
150997	2.353	4800	2.2	2	0.67	2.503±0.018	0.64	2.493±0.018	0.7	78.8
156283	4.674	4163	1.42	10	0.76	5.178±0.011	0.74	5.159±0.011	0.2	53.9
159561	1.778	8500	3.3	2	0.45	1.848±0.012	0.49	1.855±0.012	0.6	94.3
161096	4.228	4390	2.0	2	0.73	4.525±0.011	0.71	4.511±0.011	0.2	69.5
161797	1.808	5454	3.82	11	0.61	1.880±0.008	0.61	1.880±0.008	0.4	150.7

Table 4 continued on next page

Table 4 (*continued*)

Target	θ_{UD}	T_{eff}	$\log g$	Initial	θ_{LD}	Final	θ_{LD}	σ_{LD}	Max SF	
	HD	(mas)	(K)		(cm s ⁻²)	Ref	μ_λ	(mas)	μ_λ	(mas)
163917	2.651	4660	2.1	2	0.70	2.810 ± 0.005	0.65	2.789 ± 0.005	0.2	120.9
169414	2.804	4467	2.24	3	0.71	2.946 ± 0.024	0.71	2.946 ± 0.024	0.8	120.5
170693	1.952	4467	2.01	3	0.69	2.056 ± 0.009	0.66	2.048 ± 0.009	0.4	120.0
172167	3.198	9333	3.98	3	0.42	3.284 ± 0.002	0.41	3.280 ± 0.016	0.5	96.6
176524	1.705	4520	2.55	9	0.71	1.814 ± 0.027	0.64	1.797 ± 0.027	1.5	120.8
176678	2.297	4500	2.1	2	0.71	2.467 ± 0.012	0.70	2.463 ± 0.012	0.5	118.4
180610	1.526	4571	2.75	3	0.71	1.637 ± 0.028	0.68	1.630 ± 0.028	1.7	120.9
181276	2.028	4660	2.1	2	0.70	2.158 ± 0.008	0.65	2.143 ± 0.008	0.4	120.5
183439	4.111	3690	1.3	2	0.81	4.439 ± 0.020	0.76	4.403 ± 0.020	0.5	69.2
186791	6.667	4246	1.52	12	0.73	7.054 ± 0.080	0.75	7.056 ± 0.080	1.1	46.3
187642	3.270	7586	4.14	3	0.51	3.309 ± 0.006	0.51	3.309 ± 0.006	0.2	117.1
187929	1.724	5826	1.50	5	0.54	1.804 ± 0.005	0.54	1.804 ± 0.007	0.4	120.8
188310	1.570	4786	2.49	3	0.67	1.671 ± 0.025	0.61	1.658 ± 0.025	1.5	118.8
196094	4.087	4310	0.64	4	0.73	4.407 ± 0.017	0.83	4.472 ± 0.017	0.4	34.3
203504	2.179	4677	2.48	3	0.70	2.315 ± 0.023	0.70	2.315 ± 0.023	1.0	120.4
204867	2.584	5370	1.3	2	0.59	2.715 ± 0.009	0.56	2.704 ± 0.009	0.3	116.8
206952	1.715	4571	2.41	3	0.72	1.847 ± 0.015	0.61	1.819 ± 0.015	0.8	120.8
209750	2.903	5190	1.2	2	0.62	3.078 ± 0.036	0.59	3.066 ± 0.036	1.2	79.6
211388	3.127	4260	2.15	13	0.74	3.371 ± 0.049	0.74	3.371 ± 0.049	1.5	78.7
212496	1.801	4700	2.2	2	0.66	1.957 ± 0.037	0.66	1.957 ± 0.037	1.9	119.1
213311	5.375	3700	0.14	14+4	0.82	5.881 ± 0.022	0.82	5.881 ± 0.022	0.4	34.3
215182	3.270	5248	2.40	3	0.61	3.454 ± 0.027	0.65	3.471 ± 0.027	0.8	34.3
218329	3.918	3540	0.8	2	0.83	4.268 ± 0.009	0.78	4.234 ± 0.009	0.2	80.1
219215	4.776	3540	0.8	2	0.83	5.230 ± 0.029	0.82	5.221 ± 0.029	0.6	53.0
219449	2.087	4571	2.42	3	0.71	2.230 ± 0.031	0.68	2.220 ± 0.031	1.4	100.0
219615	2.358	5012	2.74	3	0.63	2.478 ± 0.012	0.64	2.482 ± 0.012	0.5	116.7
222404	3.041	4786	3.20	3	0.69	3.254 ± 0.020	0.69	3.254 ± 0.020	0.6	81.1

NOTE—The errors on the UD diameter are the same as those on the LD diameter. The initial μ_λ is based on the T_{eff} and g listed in the table, and the final μ_λ is based on the new T_{eff} determination. (See Section 3.2 for more details). The T_{eff} and $\log g$ come from the following sources: 1. Prugniel et al. (2007); 2. Lafrasse et al. (2010); 3. Allende Prieto & Lambert (1999); 4. Cox (2000) based on the star's SIMBAD spectral type; 5. Le Borgne et al. (2003); 6. Houdashelt et al. (2000); 7. Katz et al. (2011); 8. Valdes et al. (2004); 9. Soubiran et al. (2016); 10. Milone et al. (2011); 11. Prugniel et al. (2011); 12. Bordé et al. (2002); 13. Hekker & Meléndez (2007); and 14. Hohle et al. (2010). Max SF is the maximum spatial frequency for that star's diameter measurement.

Table 5. Derived Stellar Parameters.

Target HD	Spectral Type	R (R_{\odot})	σ_R (%)	F_{BOL} (10^{-6} erg s $^{-1}$ cm $^{-2}$)	A_V (mag)	T_{eff} (K)	σ_T (%)	L (L_{\odot})
432	F2 III	3.79±0.04	1.0	3.04±0.15	0.00±0.01	6739±88	1.3	26.8±1.4
1013	M2 III	52.88± ^{1.37} _{1.31}	2.6	1.38±0.07	0.31±0.01	3842±49	1.3	549.9±38.8
1522	K1 III	29.95± ^{0.72} _{0.73}	2.4	1.70±0.09	0.39±0.01	4645±73	1.6	376.8±22.0
8512	K0 III	10.37±0.09	0.9	1.53±0.08	0.28±0.02	4951±64	1.3	58.3±3.0
9927	K3 III	21.30±0.21	1.0	1.54±0.08	0.00±0.01	4316±54	1.3	142.1±7.6
17709	K5 III	60.16± ^{3.58} _{4.06}	6.7	1.32±0.07	0.40±0.02	4014±51	1.3	847.5±114.9
18925	G8 III	31.21± ^{1.15} _{1.24}	4.0	2.24±0.11	0.00±0.02	4589±58	1.3	389.6±35.5
20644	K3 III	65.70± ^{2.66} _{2.89}	4.4	1.82±0.17	1.13±0.02	4485±108	2.4	1576±199
28305	G8 III	12.53±0.28	2.2	1.27±0.06	0.00±0.18	4880±77	1.6	80.3±4.4
31964	A2 I	see note 1	-	6.59±0.96	1.58±0.02	7977±292	3.7	see note 2
34085	B8 I	74.1± ^{6.1} _{7.3}	10	28.10±1.41	0.00±0.01	10556±133	1.3	61515±11486
38944	M0 III	74.2± ^{7.0} _{8.7}	12	1.45±0.07	0.57±0.02	3912±52	1.3	1165±250
43232	K1 III	50.82± ^{1.54} _{1.62}	3.2	1.71±0.09	0.82±0.01	4810±66	1.4	1247±96
48329	G8 I	130.22± ^{5.51} _{6.01}	4.6	4.59±0.23	0.92±0.02	5009±63	1.3	9636±976
58207	G8 III	9.48±0.12	1.2	1.26±0.06	0.31±0.02	5072±68	1.3	53.7±2.8
62345	G8 III	11.00±0.16	1.4	1.18±0.06	0.00±0.01	5020±68	1.4	69.3±3.7
62509	K0 III	9.06±0.03	0.3	9.75±0.49	0.00±0.01	4586±57	1.3	32.7±1.6
66141	K2 III	22.99± ^{0.55} _{0.56}	2.4	1.05±0.05	0.52±0.02	4521±65	1.4	199.2±12.6
69267	K4 III	51.66± ^{0.96} _{0.99}	1.9	2.50±0.13	0.23±0.01	4094±53	1.3	676.7±41.4
70272	K4 III	53.27± ^{1.55} _{1.64}	3.1	1.82±0.09	0.63±0.02	4181±54	1.3	782.4±60.3
76294	G8 III	17.61±0.19	1.1	2.12±0.05	0.19±0.02	4996±30	0.6	174.2±9.3
82308	K4 III	44.93± ^{0.85} _{0.87}	1.9	1.70±0.09	0.59±0.02	4152±53	1.3	541.4±33.5
82328	F7 V	2.41±0.02	0.8	1.41±0.07	0.00±0.00	6256±82	1.3	8.0±0.4
83618	K2 III	30.03± ^{0.44} _{0.45}	1.5	1.94±0.10	0.70±0.02	4695±63	1.3	395.3±21.7
84441	G0 III	21.03± ^{0.31} _{0.32}	1.5	2.23±0.11	0.30±0.01	5623±75	1.3	399.1±21.9
85503	K2 III	11.81±0.10	0.8	1.25±0.06	0.28±0.01	4606±59	1.3	56.6±2.9
87901	B6 IV	4.35±0.10	2.4	17.10±0.86	0.10±0.01	11668±195	1.7	316.2±16.7
94264	K0 III	8.21±0.06	0.7	1.21±0.06	0.24±0.02	4790±60	1.3	32.0±1.6
95689	G9 III	17.03±0.13	0.7	8.66±0.43	0.37±0.01	5012±65	1.3	165.1±8.3

Table 5 continued on next page

Table 5 (*continued*)

Target	Spectral	<i>R</i>	σ_R	<i>F_{BOL}</i>	<i>A_V</i>	<i>T_{eff}</i>	σ_T	<i>L</i>
HD	Type	(<i>R_⊕</i>)	(%)	(10^{-6} erg s ⁻¹ cm ⁻²)	(mag)	(K)	(%)	(<i>L_⊕</i>)
96833	K1 III	19.67±0.13	0.6	2.56±0.13	0.21±0.01	4606±58	1.3	157.2±8.1
97778	M3 II	195.4± ^{31.4} _{46.2}	24	2.17±0.11	0.00±0.02	3613±48	1.3	see note 2
98262	K3 III	60.00± ^{1.24} _{1.29}	2.2	2.65±0.13	0.48±0.02	4422±56	1.3	1242±81
100029	M0 III	69.99± ^{1.06} _{1.10}	1.6	2.71±0.14	0.40±0.01	3761±47	1.3	884.4±52
102212	M1 III	54.77± ^{0.88} _{0.91}	1.7	2.06±0.10	0.10±0.01	3728±47	1.3	523.0±31.2
108381	K1 III	12.01± ^{0.33} _{0.34}	2.8	0.75±0.04	0.21±0.02	4660±84	1.8	61.4±3.3
108907	M3 III	111.0± ^{9.3} _{11.2}	10	1.87±0.14	0.50±0.04	3718±69	1.9	2122±419
109358	G0 V	1.03±0.03	3.0	0.54±0.03	0.04±0.01	5966±117	2.0	1.2±0.1
113226	G8 III	11.98±0.07	0.6	2.33±0.12	0.00±0.01	5020±64	1.3	82.3±4.2
113996	K5 III	33.75± ^{0.77} _{0.80}	2.4	1.00±0.05	0.30±0.02	4211±54	1.3	323.0±21.7
117675	M2 III	78.38± ^{1.90} _{1.98}	2.5	1.77±0.09	0.46±0.02	3500±46	1.3	831.5±56.8
120136	F7 IV-V	1.38±0.08	6.0	0.42±0.02	0.00±0.01	6556±212	3.2	3.2±0.2
120315	B3 V	3.4±0.5	15	18.70±0.94	0.04±0.01	15540±1157	7.4	594.0±31.1
120477	K5 III	40.72± ^{0.77} _{0.79}	2.0	1.90±0.10	0.30±0.02	4012±51	1.3	387.8±24.2
120933	M3 III	117.41± ^{4.25} _{4.57}	3.9	2.25±0.11	0.58±0.02	3722±48	1.3	2387±213
121130	M3 III	83.22± ^{2.08} _{2.16}	2.6	2.54±0.13	0.50±0.02	3584±35	1.0	1031±70
127665	K3 III	20.58±0.19	0.9	1.71±0.09	0.11±0.01	4285±54	1.3	128.9±6.8
129712	M3 III	129.36± ^{7.49} _{8.42}	6.5	1.92±0.10	0.49±0.02	3691±50	1.3	2802±367
133124	K4 III	37.39± ^{1.49} _{1.55}	4.1	0.88±0.04	0.38±0.02	4106±73	1.8	358.7±29.1
133208	G8 III	18.44±0.19	1.0	1.26±0.06	0.00±0.01	4976±63	1.3	188.0±10.1
136726	K4 III	28.20± ^{0.71} _{0.73}	2.6	0.56±0.03	0.00±0.04	4358±59	1.4	258.8±17.7
137759	K2 III	11.87±0.05	0.4	2.16±0.11	0.18±0.02	4756±60	1.3	65.0±3.3
140573	K2 III	11.62±0.06	0.5	3.66±0.18	0.13±0.01	4687±59	1.3	58.9±3.0
143107	K2 III	21.87± ^{0.98} _{0.99}	4.5	1.13±0.06	0.34±0.01	4408±109	2.5	162.9±9.4
148387	G8 III	10.53±0.04	0.4	2.63±0.13	0.00±0.02	5060±64	1.3	65.6±3.3
148856	G5 III	15.92± ^{0.39} _{0.41}	2.5	2.70±0.14	0.17±0.02	5092±64	1.3	153.7±10.8
150997	G5 III	8.92±0.07	0.8	1.32±0.07	0.09±0.02	5025±65	1.3	45.8±2.3
156283	K3-4 II	64.02± ^{0.89} _{0.91}	1.4	2.82±0.14	0.00±0.02	4223±53	1.3	1176±67
159561	A4-7 III	2.97±0.05	1.7	3.88±0.19	0.09±0.01	7627±98	1.3	26.9±1.6
161096	K2 III	12.17±0.06	0.5	2.93±0.15	0.05±0.01	4559±57	1.3	57.7±2.9
161797	G5 IV	1.64±0.01	0.4	1.02±0.05	0.00±0.00	5425±69	1.3	2.1±0.1

Table 5 continued on next page

Table 5 (*continued*)

Target	Spectral	<i>R</i>	σ_R	F_{BOL}	A_V	T_{eff}	σ_T	<i>L</i>
HD	Type	(R_\odot)	(%)	(10^{-6} erg s $^{-1}$ cm $^{-2}$)	(mag)	(K)	(%)	(L_\odot)
163917	G8 III	13.85±0.17	1.2	1.62±0.08	0.16±0.01	5000±63	1.3	108.2±6.0
169414	K2 III	11.55± ^{0.19} _{0.20}	1.7	1.26±0.06	0.14±0.02	4569±60	1.3	52.4±3.0
170693	K1 III	21.25± ^{0.41} _{0.43}	2.0	0.69±0.06	0.54±0.04	4714±101	2.1	201.1±18.8
172167	A0 V	2.71±0.02	0.6	28.80±1.44	0.00±0.01	9467±121	1.3	53.1±2.7
176524	K0 III	20.37± ^{0.97} _{1.06}	5.2	0.76±0.07	0.72±0.03	5148±126	2.4	263.1±35.0
176678	K1 III	11.68±0.13	1.1	0.96±0.05	0.12±0.02	4662±59	1.3	58.2±3.1
180610	K2 III	8.87±0.17	1.9	0.50±0.05	0.25±0.06	4868±124	2.6	39.9±3.9
181276	G8 III	8.77±0.05	0.5	1.00±0.05	0.03±0.02	5056±64	1.3	45.3±2.3
183439	M0 III	43.14± ^{1.09} _{1.15}	2.7	1.60±0.08	0.31±0.02	3967±50	1.3	415.9±29.7
186791	K3-4 II	91.81± ^{2.12} _{2.19}	2.4	4.68±0.23	0.15±0.01	4098±56	1.4	2146±139
187642	A7 V	1.82±0.01	0.3	12.30±0.62	0.01±0.01	7620±95	1.3	10.1±0.5
187929	G0 III	see note 1	-	1.74±0.14	0.63±0.03	6329±126	2.0	see note 2
188310	G8 III	10.03±0.22	2.2	0.70±0.05	0.55±0.03	5263±105	2.0	69.6±5.6
196094	K4 I	see note 1	-	1.21±0.40	0.00±1.91	3671±304	8.3	see note 2
203504	K1 III	11.89±0.15	1.3	0.89±0.04	0.10±0.02	4725±64	1.3	63.5±3.3
204867	G0 I	47.88± ^{1.68} _{1.81}	3.8	2.41±0.12	0.36±0.01	5608±71	1.3	2046±180
206952	K0 III	10.93± ^{0.26} _{0.27}	2.4	0.97±0.08	0.69±0.03	5446±113	2.1	94.9±8.8
209750	G2 I	52.89± ^{1.68} _{1.78}	3.4	2.63±0.13	0.42±0.01	5383±74	1.4	2120±167
211388	K3 III	69.01± ^{3.07} _{3.32}	4.8	1.28±0.06	0.45±0.01	4288±62	1.4	1453±147
212496	G8 III	10.96±0.23	2.1	0.68±0.03	0.26±0.01	4803±75	1.6	57.7±3.0
213311	K4 I	319.2± ^{26.6} _{32.0}	10	2.19±0.13	0.10±0.29	3713±56	1.5	17473±3344
215182	G2 III	24.51± ^{1.11} _{1.21}	5.0	2.45±0.12	0.29±0.01	4970±65	1.3	330.8±35.0
218329	M1 III	45.87± ^{1.31} _{1.38}	3.0	1.52±0.08	0.30±0.01	3994±50	1.3	483.1±37.2
219215	M1 III	34.77± ^{1.83} _{2.04}	5.9	1.73±0.09	0.17±0.01	3715±48	1.3	207.7±25.2
219449	K1 III	10.96±0.21	1.9	0.82±0.04	0.16±0.01	4730±68	1.4	54.3±3.1
219615	G8 III	11.28±0.10	0.9	1.12±0.06	0.00±0.02	4833±62	1.3	62.7±3.3
222404	K1 III	4.93±0.04	0.8	1.86±0.09	0.00±0.02	4792±62	1.3	11.6±0.6

NOTE—The spectral types are those that provide the best SED fit as described in Section 3.2. The SED fits are also the source of F_{BOL} and A_V . The other parameters are derived as described in Section 3.2. Note 1: The large error on the parallax measurement made the radius determination unuseful, considering the error would be more than 50%. Note 2: Because the errors on the parallax measurements are unusually high ($\geq 20\%$), the errors on the subsequent luminosity calculations render them unhelpful for these stars.

Table 6. Stellar Masses and Ages.

Target	Mass	Age
HD	(M_{\odot})	(Gyr)
432	2.02±0.03	1.00±0.05
1013	1.06±0.11	7.70±2.01
1522	3.70±0.10	0.23±0.03
8512	2.06±0.14	1.08±0.23
9927	1.75±0.15	1.70±0.40
17709	1.34±0.18	3.10±1.20
18925	3.64±0.25	0.23±0.05
20644	3.07±0.39	0.35±0.14
28305	2.69±0.11	0.55±0.10
31964	2.16±0.39	0.62±0.22
38944	1.64±0.22	1.98±0.68
43232	4.19±0.14	0.17±0.02
48329	5.29±0.04	0.10±0.00
58207	2.09±0.10	0.96±0.15
62345	2.58±0.09	0.58±0.08
62509	0.98±0.10	7.66±2.08
66141	1.59±0.19	1.89±0.64
69267	1.75±0.11	1.49±0.22
70272	1.95±0.18	1.32±0.23
76294	3.09±0.10	0.37±0.04
82308	1.29±0.18	3.62±1.37
83618	2.82±0.32	0.46±0.17
84441	3.71±0.04	0.21±0.00
85503	1.58±0.14	2.15±0.50
87901	3.57±0.04	0.16±0.01
94264	1.54±0.10	2.29±0.42
95689	3.44±0.11	0.28±0.03
96833	2.37±0.15	0.68±0.14
97778	3.11±0.69	0.40±0.24
98262	3.82±0.23	0.20±0.03
100029	1.53±0.12	2.33±0.48
102212	0.92±0.00	11.69±0.13
108381	1.78±0.25	1.69±0.56
108907	1.64±0.20	1.97±0.57
113226	2.96±0.09	0.38±0.04
113996	1.21±0.19	4.51±1.84
117675	1.40±0.12	2.90±0.68
120477	1.00±0.05	10.08±1.41

Table 6 continued on next page

Table 6 (*continued*)

Target HD	Mass (M_{\odot})	Age (Gyr)
120933	2.18±0.16	1.11±0.21
121130	0.93±0.06	10.24±1.40
127665	1.29±0.12	4.31±1.17
129712	2.20±0.23	1.05±0.27
133124	1.50±0.20	2.56±0.92
133208	3.33±0.06	0.30±0.02
136726	2.04±0.20	1.21±0.33
137759	1.75±0.17	1.70±0.33
140573	1.61±0.12	2.06±0.33
143107	1.37±0.24	3.24±1.81
148387	2.45±0.10	0.65±0.10
148856	2.91±0.11	0.42±0.06
150997	2.01±0.11	1.08±0.18
156283	3.77±0.20	0.22±0.04
159561	1.93±0.03	0.91±0.03
161096	1.44±0.16	2.75±0.78
161797	1.09±0.01	7.68±0.13
163917	2.98±0.11	0.39±0.05
169414	1.05±0.18	6.39±2.71
170693	1.54±0.24	1.93±0.91
176524	3.01±0.12	0.40±0.06
176678	1.28±0.18	3.64±1.43
180610	1.65±0.25	1.97±0.94
181276	2.45±0.11	0.61±0.08
183439	0.97±0.02	11.30±0.54
186791	3.51±0.23	0.27±0.04
187929	4.24±0.58	0.15±0.05
188310	2.05±0.15	0.98±0.18
196094	4.49±0.66	0.15±0.06
203504	1.60±0.18	2.04±0.54
204867	4.97±0.10	0.11±0.01
206952	2.38±0.07	0.67±0.06
209750	5.13±0.06	0.10±0.00
211388	4.16±0.28	0.17±0.03
212496	0.97±0.21	6.76±3.59
213311	5.11±0.18	0.11±0.01
215182	3.51±0.13	0.27±0.03
218329	1.61±0.13	2.13±0.46
219215	1.00±0.03	10.97±0.83
219449	1.38±0.29	2.98±1.63
219615	1.11±0.29	4.58±3.10

Table 6 continued on next page

Table 6 (*continued*)

Target	Mass	Age
HD	(M_{\odot})	(Gyr)
222404	1.41±0.08	3.25±0.63

NOTE—Masses and ages were determined using the PARAM stellar model described in Section 3.3. An error of 0.05 was assigned to [Fe/H] (a model input), which are from the sources listed in Table 1.

Table 7. Interferometric Angular Diameter Comparison.

Target	$\theta_{LD, \text{here}}$		Reference
	HD	(mas)	
432	2.103±0.015	2.218±0.058	Hutter et al. (2016)
		1.698±0.023	Che et al. (2011)
		2.12±0.05	Nordgren et al. (1999)
1013	4.359±0.022	N/A	N/A
1522	3.310±0.062	3.325±0.010	Richichi et al. (2009)
8512	2.764±0.016	2.817±0.044	Richichi et al. (2009)
9927	3.649±0.007	3.76±0.07	Nordgren et al. (1999)
17709	3.907±0.021	4.056±0.041	Mozurkewich et al. (2003)
18925	3.894±0.018	N/A	N/A
20644	3.674±0.025	N/A	N/A
28305	2.592±0.050	2.733±0.031	Boyajian et al. (2009)
		2.481±0.045	van Belle & von Braun (2009)
		2.671±0.049	Mozurkewich et al. (2003)
		2.41±0.11	Nordgren et al. (2001)
		2.67±0.04	Nordgren et al. (2001)
		2.51±0.06*	van Belle et al. (1999)
31964	2.210±0.012	2.20±0.02	Mourard et al. (2012)
		2.27±0.11*	Stencel et al. (2008)
		2.096±0.086	Mozurkewich et al. (2003)
		2.28±0.09	Nordgren et al. (2001)
		2.17±0.03	Nordgren et al. (2001)
34085	2.606±0.009	2.914±0.179	Richichi et al. (2009)
		2.55±0.05	Hanbury Brown et al. (1974a)
		2.69±0.15	Hanbury Brown (1968)
38944	4.310±0.036	N/A	N/A
43232	3.097±0.034	N/A	N/A
48329	4.677±0.013	4.703±0.047	Mozurkewich et al. (2003)
		4.77±0.05	Nordgren et al. (2001)
		4.78±0.07	Nordgren et al. (2001)
58207	2.390±0.024	N/A	N/A
62345	2.361±0.025	N/A	N/A
62509	8.134±0.013	8.018±0.043	Hutter et al. (2016)
		8.170±0.444	van Belle & von Braun (2009)
		7.980±0.080	Mozurkewich et al. (2003)
		7.95±0.09	Nordgren et al. (2001)
		7.97±0.11	Nordgren et al. (2001)
		8.035±0.08	Mozurkewich et al. (1991)
		9.26±0.15	Shao et al. (1988)
		7.90±0.31	di Benedetto & Rabbia (1987)

Table 7 continued on next page

Table 7 (*continued*)

Target	$\theta_{\text{LD,here}}$	$\theta_{\text{LD,previous}}$	Reference
HD	(mas)	(mas)	
66141	2.747±0.039	N/A	N/A
69267	5.167±0.035	5.238±0.069 5.13±0.06 5.20±0.07	Mozurkewich et al. (2003) Nordgren et al. (2001) Nordgren et al. (2001)
70272	4.228±0.024	N/A	N/A
76294	3.196±0.017	3.29±0.08 3.18±0.09	Nordgren et al. (2001) Nordgren et al. (2001)
82308	4.143±0.025	N/A	N/A
82328	1.664±0.012	1.632±0.005	Boyajian et al. (2012a)
83618	3.462±0.033	3.451±0.042	Richichi et al. (2009)
84441	2.587±0.025	2.575±0.078 2.70±0.10 2.60±0.05	Mozurkewich et al. (2003) Nordgren et al. (2001) Nordgren et al. (2001)
85503	2.887±0.016	N/A	N/A
87901	1.664±0.037	1.234±0.010 1.209±0.053 1.65±0.02 1.37±0.06 1.38±0.07	Che et al. (2011) van Belle & von Braun (2009) McAlister et al. (2005) Hanbury Brown et al. (1974a) Hanbury Brown et al. (1967)
94264	2.622±0.009	2.462±0.054 2.54±0.03	Hutter et al. (2016) Nordgren et al. (1999)
95689	6.419±0.041	6.739±0.099 6.91±0.08 7.11±0.10	Mozurkewich et al. (2003) Nordgren et al. (2001) Nordgren et al. (2001)
96833	4.131±0.007	4.120±0.041 4.08±0.07 4.12±0.06	Mozurkewich et al. (2003) Nordgren et al. (2001) Nordgren et al. (2001)
97778	6.182±0.057	5.7±0.6*	Dyck et al. (1998)
98262	4.561±0.016	4.759±0.048 4.76±0.07 4.71±0.07	Mozurkewich et al. (2003) Nordgren et al. (2001) Nordgren et al. (2001)
100029	6.376±0.012	6.430±0.069 6.37±0.07 6.47±0.09 7.3±0.7*	Mozurkewich et al. (2003) Nordgren et al. (2001) Nordgren et al. (2001) Dyck et al. (1998)
102212	5.657±0.013	6.116±0.115 5.65±0.07 6.26±0.10	Mozurkewich et al. (2003) Nordgren et al. (2001) Nordgren et al. (2001)
108381	2.179±0.057	N/A	N/A
108907	5.420±0.010	N/A	N/A
109358	1.133±0.034	1.238±0.030	Boyajian et al. (2012a)

Table 7 continued on next page

Table 7 (*continued*)

Target	$\theta_{\text{LD,here}}$	$\theta_{\text{LD,previous}}$	Reference
HD	(mas)	(mas)	
		1.138±0.055	van Belle & von Braun (2009)
113226	3.318±0.013	3.062±0.030*	van Belle et al. (2013)
		3.283±0.033	Mozurkewich et al. (2003)
		3.23±0.05	Nordgren et al. (2001)
		3.28±0.05	Nordgren et al. (2001)
		3.17±0.03	Nordgren et al. (1999)
113996	3.090±0.019	N/A	N/A
117675	5.951±0.049	N/A	N/A
120136	0.822±0.049	0.786±0.016	Baines et al. (2008)
120315	0.981±0.144	N/A	N/A
120477	4.691±0.022	4.72±0.05	Nordgren et al. (1999)
120933	5.932±0.042	N/A	N/A
121130	6.799±0.077	N/A	N/A
127665	3.901±0.008	3.72±0.12*	van Belle et al. (1999)
129712	5.573±0.055	N/A	N/A
133124	3.055±0.077	N/A	N/A
133208	2.484±0.008	2.477±0.065	Mozurkewich et al. (2003)
		2.48±0.08	Nordgren et al. (2001)
		2.47±0.04	Nordgren et al. (2001)
136726	2.149±0.023	2.366±0.020	Baines et al. (2010)
137759	3.559±0.011	3.596±0.015	Baines et al. (2011)
140573	4.770±0.013	4.807±0.035	Hutter et al. (2016)
		4.846±0.048	Mozurkewich et al. (2003)
		4.83±0.09	Nordgren et al. (2001)
		4.78±0.07	Nordgren et al. (2001)
143107	2.997±0.128	N/A	N/A
148387	3.470±0.010	3.355±0.077	Hutter et al. (2016)
		3.722±0.071	Mozurkewich et al. (2003)
		3.34±0.07	Nordgren et al. (2001)
		3.68±0.05	Nordgren et al. (2001)
148856	3.472±0.008	3.462±0.035	Mozurkewich et al. (2003)
		3.53±0.08	Nordgren et al. (2001)
		3.51±0.05	Nordgren et al. (2001)
150997	2.493±0.018	2.624±0.034	Mozurkewich et al. (2003)
		2.50±0.08	Nordgren et al. (2001)
		2.64±0.04	Nordgren et al. (2001)
		2.42±0.07	Nordgren et al. (1999)
156283	5.519±0.011	5.275±0.067	Mozurkewich et al. (2003)
		5.26±0.06	Nordgren et al. (2001)
		5.27±0.07	Nordgren et al. (2001)
		5.20±0.03	Nordgren et al. (1999)

Table 7 continued on next page

Table 7 (*continued*)

Target	$\theta_{\text{LD,here}}$	$\theta_{\text{LD,previous}}$	Reference
HD	(mas)	(mas)	
159561	1.855±0.012	1.514±0.004	Monnier et al. (2010)
		1.63±0.013	Hanbury Brown et al. (1974a)
161096	4.511±0.011	4.43±0.01	Chiavassa et al. (2017)
		4.498±0.032	Hutter et al. (2016)
161797	1.880±0.008	1.957±0.012	Baines et al. (2014)
		1.953±0.039	Mozurkewich et al. (2003)
163917	2.789±0.005	N/A	N/A
169414	2.946±0.024	N/A	N/A
170693	2.048±0.009	2.097±0.009	Ligi et al. (2016)
		2.12±0.02	Ligi et al. (2012)
		2.041±0.043	Baines et al. (2010)
172167	3.280±0.016	2.930±0.007	Monnier et al. (2012)
		3.08±0.03*	Mourard et al. (2009)
		3.202±0.005*	Absil et al. (2006)
		3.329±0.006	Aufdenberg et al. (2006)
		3.225±0.032	Mozurkewich et al. (2003)
		3.28±0.01	Ciardi et al. (2001)
		3.24±0.07	Hanbury Brown et al. (1974a)
		3.47±0.16	Hanbury Brown et al. (1967)
176524	1.797±0.027	N/A	N/A
176678	2.463±0.012	N/A	N/A
180610	1.630±0.028	N/A	N/A
181276	2.143±0.008	2.07±0.09	Nordgren et al. (1999)
183439	4.403±0.020	4.458±0.045	Mozurkewich et al. (2003)
186791	7.056±0.080	7.271±0.073	Mozurkewich et al. (2003)
		7.16±0.08	Nordgren et al. (2001)
		7.24±0.10	Nordgren et al. (2001)
		7.08±0.05	Nordgren et al. (1999)
187642	3.309±0.006	3.346±0.230	Richichi et al. (2009)
		3.670±0.007	Monnier et al. (2007)
		3.327±0.017	Peterson et al. (2006)
		3.258±0.034	Domiciano de Souza et al. (2005)
		3.32±0.11	Ohishi et al. (2004)
		3.462±0.035	Mozurkewich et al. (2003)
		3.461±0.038	van Belle et al. (2001)
		2.98±0.14	Hanbury Brown et al. (1974a)
		2.97±0.15	Hanbury Brown et al. (1967)
187929	1.804±0.007	1.793±0.070	Lane et al. (2002)
		1.69±0.04	Armstrong et al. (2001)
		1.73±0.05	Nordgren et al. (1999)
188310	1.658±0.025	1.726±0.008	Baines et al. (2009)

Table 7 continued on next page

Table 7 (*continued*)

Target	$\theta_{\text{LD,here}}$	$\theta_{\text{LD,previous}}$	Reference
HD	(mas)	(mas)	
196094	4.472±0.017	N/A	N/A
203504	2.315±0.023	N/A	N/A
204867	2.704±0.009	N/A	N/A
206952	1.819±0.015	N/A	N/A
209750	3.066±0.036	3.237±0.057 3.11±0.04 3.20±0.05 3.08±0.03	Mozurkewich et al. (2003) Nordgren et al. (2001) Nordgren et al. (2001) Nordgren et al. (1999)
211388	3.371±0.049	N/A	N/A
212496	1.957±0.037	1.909±0.011 1.92±0.02	Armstrong et al. (2001) Nordgren et al. (1999)
213311	5.881±0.022	N/A	N/A
215182	3.471±0.027	3.23±0.07 3.26±0.07	Nordgren et al. (2001) Nordgren et al. (2001)
218329	4.234±0.009	N/A	N/A
219215	5.221±0.029	N/A	N/A
219449	2.220±0.031	N/A	N/A
219615	2.482±0.012	N/A	N/A
222404	3.254±0.020	3.329±0.042 3.302±0.029 3.24±0.03	Hutter et al. (2016) Baines et al. (2009) Nordgren et al. (1999)

NOTE—*No LD diameter was provided, therefore we list the UD diameter here. Figure 4 shows a graphical representation of this table. If more than one diameter was available in the literature, we used the most recent one when plotting the results in Figure 4.

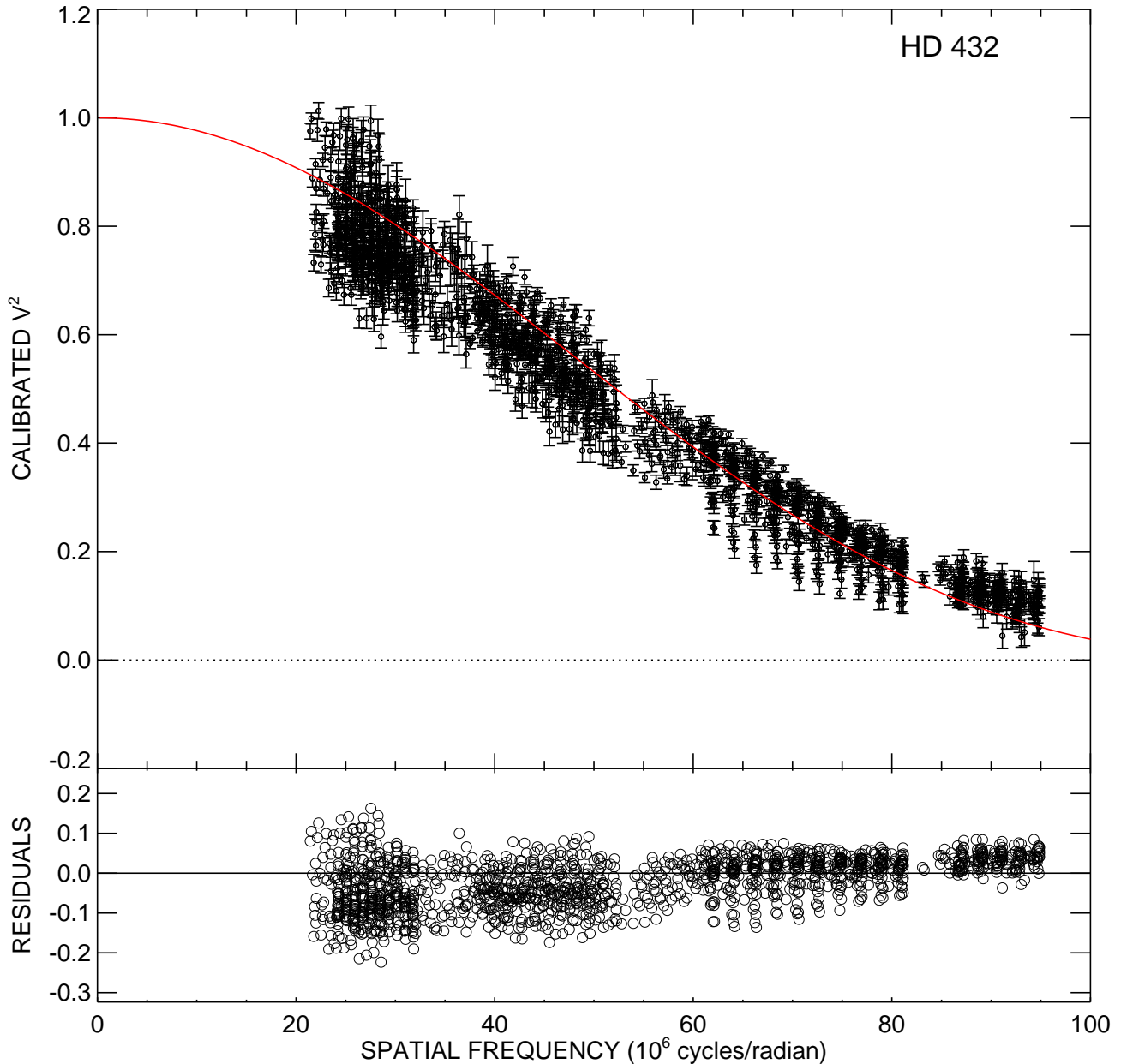


Figure 1. *Top panel:* The θ_{LD} fit for HD 432. The solid lines represent the visibility curve for the best fit θ_{LD} , the points are the calibrated visibilities, and the vertical lines are the measurement uncertainties. *Bottom panel:* The residuals (O-C) of the diameter fit to the visibilities. The plots for the remaining stars are available on the electronic version of the *Astronomical Journal*.

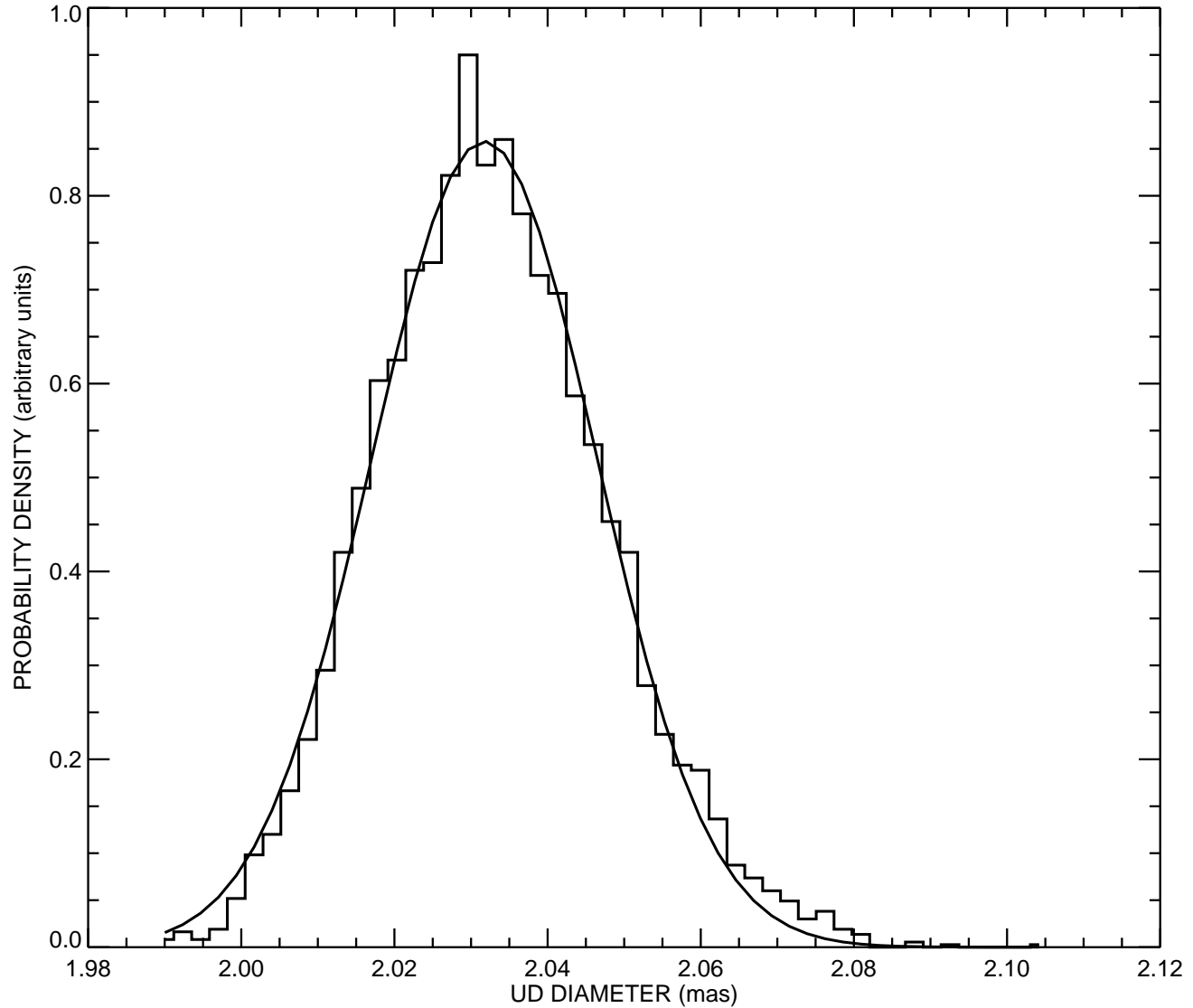


Figure 2. An example probability density solution for the diameter fit to HD 432 visibilities as described in Section 3.1.

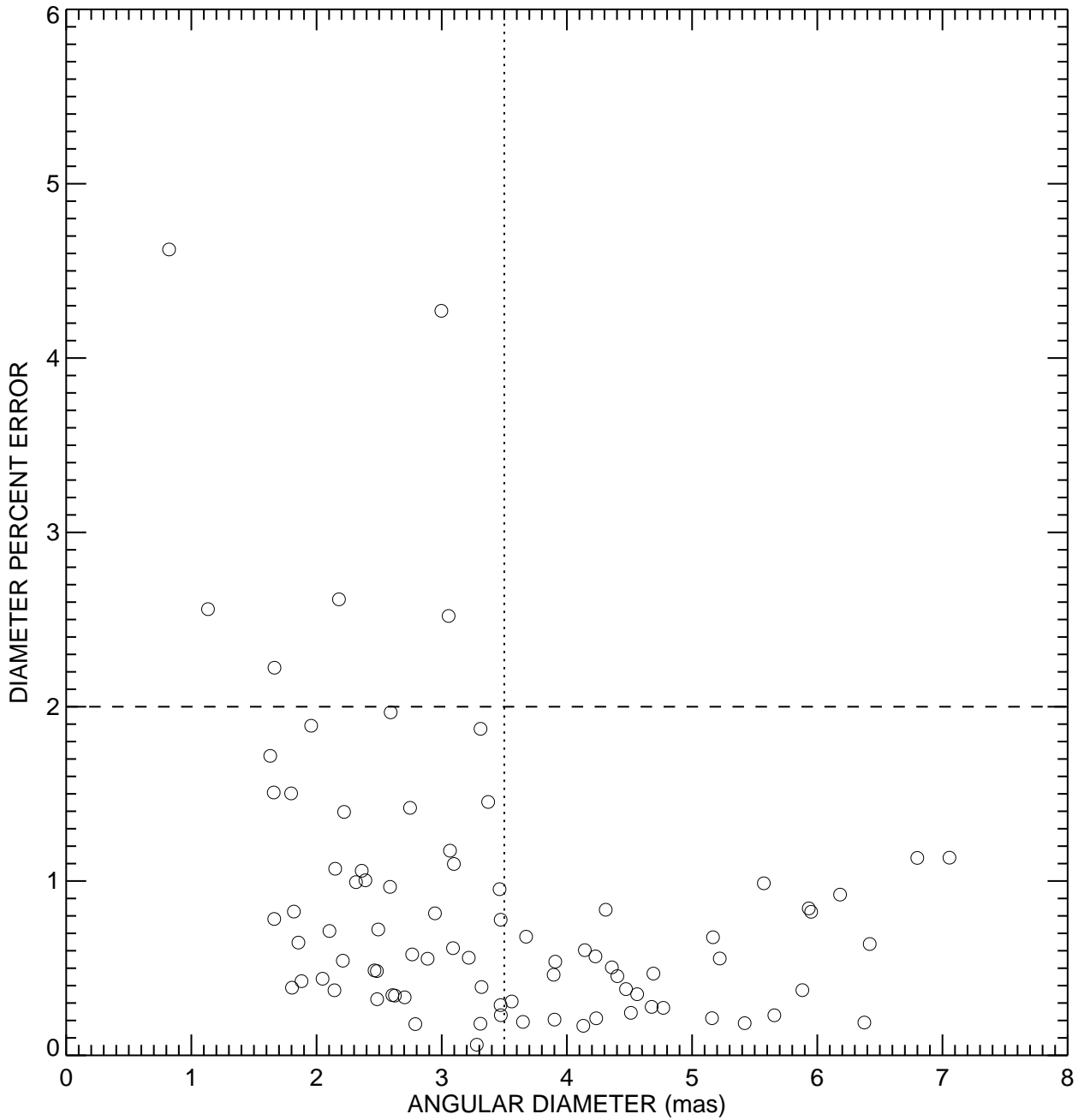


Figure 3. Characterizing the NPOI performance based on the percent error in the limb-darkened diameter measurement (σ_{LD}) versus θ_{LD} . The horizontal dashed line shows the $\sigma_{LD}=2\%$ cut-off that is the minimal standard of astrophysically useful measurements, while the vertical dotted line shows the 3.5-mas cut-off where σ_{LD} errors are $\sim 1\%$ or better. The star with the highest error (HD 120315, $\sigma_{LD} = 15\%$) is not included with this plot so that the spread of the other points is more easily visible.

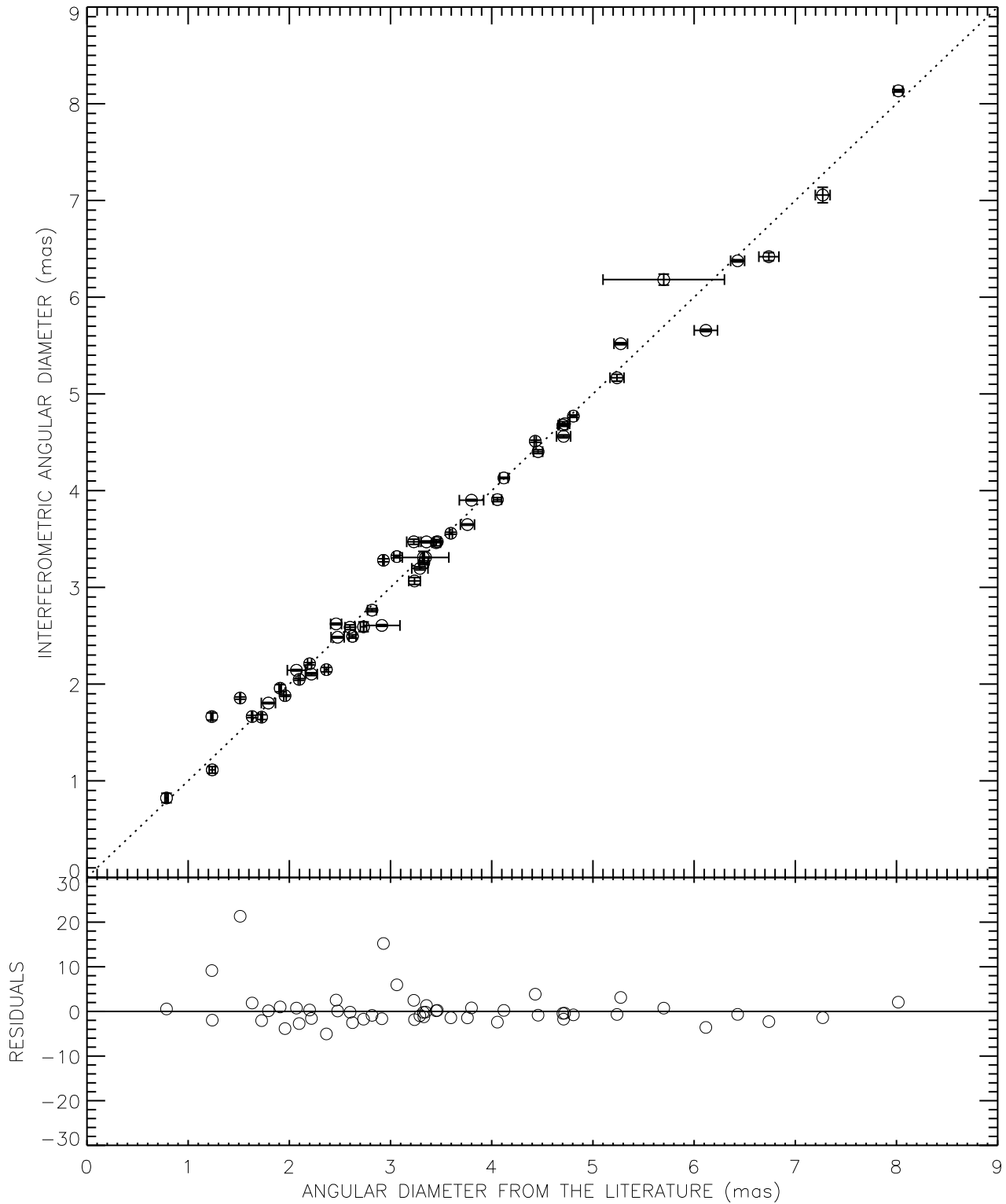


Figure 4. *Top panel:* Comparison of interferometrically measured angular diameters versus diameters from the literature. The error bars for the interferometric diameters are often smaller than the circle that indicates that measurement. The dotted line is the 1:1 ratio. When more than one measurement was available in the literature, we used the most recent measurement (see Table 7). *Bottom panel:* The residuals were calculated as follows: $(\theta_{\text{interferometry}} - \theta_{\text{literature}}) \times (\text{combined error})^{-1}$.